

# Performance of Statistical and Machine Learning-Based Methods for Predicting Biogeographical Patterns of Fungal Productivity in Forest Ecosystems

Albert Morera (✉ [morera.marra@gmail.com](mailto:morera.marra@gmail.com))

UdL: Universitat de Lleida <https://orcid.org/0000-0002-6777-169X>

Juan Martínez de Aragón

Forest Science and Technology Centre of Catalonia

José Antonio Bonet

Escola Tècnica Superior d'Enginyeria Agrària de Lleida: Universitat de Lleida Escola Tècnica Superior d'Enginyeria Agrària

Jingjing Liang

Purdue University Department of Forestry and Natural Resources

Sergio de-Miguel

Escola Tècnica Superior d'Enginyeria Agrària de Lleida: Universitat de Lleida Escola Tècnica Superior d'Enginyeria Agrària

---

## Research

**Keywords:** Artificial intelligence, Modelling, Biogeography, Climate, Forest, Fungi, Mushrooms

**Posted Date:** December 8th, 2020

**DOI:** <https://doi.org/10.21203/rs.3.rs-122045/v1>

**License:** © ⓘ This work is licensed under a Creative Commons Attribution 4.0 International License.

[Read Full License](#)

---

**Version of Record:** A version of this preprint was published on March 15th, 2021. See the published version at <https://doi.org/10.1186/s40663-021-00297-w>.

1 **Title: Performance of statistical and machine learning-based methods for predicting**  
2 **biogeographical patterns of fungal productivity in forest ecosystems**

3

4 Authors: Albert Morera<sup>1,2\*</sup>, Juan Martínez de Aragón<sup>3</sup>, José Antonio Bonet<sup>1,2</sup>, Jingjing  
5 Liang<sup>4</sup>, Sergio de-Miguel<sup>1,2</sup>

6

7 Affiliations:

8 <sup>1</sup> Department of Crop and Forest Sciences, University of Lleida, Av. Alcalde Rovira  
9 Roure 191, E-25198 Lleida, Spain

10 <sup>2</sup> Joint Research Unit CTFC – AGROTECNIO, Av. Alcalde Rovira Roure 191, E-25198  
11 Lleida, Spain

12 <sup>3</sup> Forest Science and Technology Centre of Catalonia, Ctra. Sant Llorenç de Morunys km  
13 2, 25280 Solsona, Spain

14 <sup>4</sup> Forest Advanced Computing and Artificial Intelligence Laboratory, Department of  
15 Forestry and Natural Resources, Purdue University, West Lafayette, IN 47907, USA

16 \* Corresponding author's email: [morera.marra@gmail.com](mailto:morera.marra@gmail.com)

17

18

19

20

21

22 **Abstract**

23 Background: The prediction of biogeographical patterns from a large number of driving  
24 factors with complex interactions, correlations and non-linear dependences require  
25 advanced analytical methods and modelling tools. This study compares different  
26 statistical and machine learning models for predicting fungal productivity  
27 biogeographical patterns as a case study for the thorough assessment of the performance  
28 of alternative modelling approaches to provide accurate and ecologically-consistent  
29 predictions.

30 Methods: We evaluated and compared the performance of two statistical modelling  
31 techniques, namely, generalized linear mixed models and geographically weighted  
32 regression, and four machine learning models, namely, random forest, extreme gradient  
33 boosting, support vector machine and deep learning to predict fungal productivity. We  
34 used a systematic methodology based on substitution, random, spatial and climatic  
35 blocking combined with principal component analysis, together with an evaluation of the  
36 ecological consistency of spatially-explicit model predictions.

37 Results: Fungal productivity predictions were sensitive to the modelling approach and  
38 complexity. Moreover, the importance assigned to different predictors varied between  
39 machine learning modelling approaches. Decision tree-based models increased prediction  
40 accuracy by ~7% compared to other machine learning approaches and by more than 25%  
41 compared to statistical ones, and resulted in higher ecological consistence at the landscape  
42 level.

43 Conclusions: Whereas a large number of predictors are often used in machine learning  
44 algorithms, in this study we show that proper variable selection is crucial to create robust  
45 models for extrapolation in biophysically differentiated areas. When dealing with spatial-

46 temporal data in the analysis of biogeographical patterns, climatic blocking is postulated  
47 as a highly informative technique to be used in cross-validation to assess the prediction  
48 error over larger scales. Random forest was the best approach for prediction both in  
49 sampling-like environments as well as in extrapolation beyond the spatial and climatic  
50 range of the modelling data.

51

52 **Keywords**

53 Artificial intelligence; Modelling; Biogeography; Climate; Forest; Fungi, Mushrooms

54

55

56

57

58

59

60

61

62

63

64

65

66

## 67 **1 Background**

68 Understanding the biogeographical patterns of organisms in natural ecosystems and  
69 predicting their distribution is a fundamental challenge in environmental sciences (Ehrlén  
70 and Morris, 2015). This entails a deep understanding of their distribution across space  
71 and time underpinning ecological mechanisms, which becomes increasingly complex  
72 with an increasing amount of factors driving these patterns and the possible interactions  
73 and nonlinear dependencies between them (Dixon et al., 1999; Ye et al., 2015). Such  
74 complex interrelationships require advanced data analytic methods and modelling tools  
75 to yield realistic predictions of natural ecosystem attributes and processes.

76 Statistical methods traditionally used for this purpose aim at accounting for several  
77 elements that govern these natural mechanisms, trying to reach a parsimonious and robust  
78 understanding of ecological patterns (Wood and Thomas, 1999). However, since  
79 conventional parametric approaches may over-simplify nonlinear relationships between  
80 variables and over- or under-estimate the influence of some drivers, conventional  
81 parametric approaches may result in poor predictions and/or descriptions of reality (Ye et  
82 al., 2015), especially for the analyses of large databases. To overcome potential  
83 limitations of classic statistical approaches in big data analysis, the increased computing  
84 power has led to recent considerable growth in the use of analytical methods based on  
85 artificial intelligence such as machine learning (Christin et al., 2019).

86 Machine learning algorithms are increasingly being used in species distribution and  
87 ecological niche modelling (Prasad et al., 2006; Culter et al., 2007; Hannemann et al.,  
88 2015; Liang et al. 2016; Prasad, 2018; Gobeyn et al., 2019), forest resources (Stojanova  
89 et al., 2010; Görgens et al., 2015) and climate change studies (Thuille, 2003; Bastin et al.,  
90 2019), among others. To determine to what extent these "new" methodologies can  
91 contribute to improving our understanding and prediction capacity within the field of

92 environmental sciences, comparative studies are required between those models that have  
93 been used historically and those fed by artificial intelligence algorithms (Özçelik et al.,  
94 2013; Diamantopoulou et al., 2015; Hill et al., 2016; Bonete et al., 2020). Yet, many  
95 machine learning algorithms have been developed in recent years, and each of them may  
96 be more or less appropriate depending on the specific tasks and research objectives  
97 (Thessen, 2016). This highlights the need for systematic studies allowing for discerning  
98 the most suitable methodology according to a given research objective and data. Although  
99 several studies have analysed the performance of different analytical approaches (Hill et  
100 al., 2016; Bonete et al., 2020; Mayfield et al., 2020), existing ecological research  
101 addressing systematic assessments and comparisons of alternative modelling and  
102 predictive methods is scarce, making it difficult to provide clear methodological  
103 recommendations about the suitability of different approaches. Besides, in the field of  
104 environmental sciences, often, extrapolations in biophysically differentiated areas are  
105 required, which makes it necessary to take even more into account the data spatial  
106 dependencies. Due to data spatial autocorrelation, random cross-validations lead to over-  
107 optimistic error estimates (Bahn and McGill, 2013; Micheletti et al., 2014; Juel et al.,  
108 2015; Gasch et al., 2015; Roberts et al., 2017; Meyer et al., 2018; Meyer et al., 2019a),  
109 which makes it necessary to use proper, complementary validation methods such as  
110 spatial cross-validation (Le Rest et al., 2014; Pohjankukka et al., 2017; Roberts et al.,  
111 2017; Meyer et al., 2018; Valavi et al., 2018). Moreover, spatial dependencies in the data  
112 can lead to a misinterpretation of some predictors outside the sampling range (Meyer et  
113 al., 2018, 2019a).

114 Biogeographical patterns of fungal dynamics over large scales are a highly relevant  
115 question in ecology given the key role of fungi in forest ecosystems (Stokland et al., 2012;  
116 Mohan et al., 2014), especially in fungi-tree symbiosis. However, due to their great

117 diversity and differential ecological requirements (Glassman et al., 2017), as well as the  
118 difficulty of monitoring their dynamics and the large array of potential drivers (Büntgen  
119 et al., 2013), little is known of fungal dynamics over large scales. The prediction of  
120 biogeographical patterns of fungal dynamics requires large fungal datasets with a correct  
121 taxonomic identification of the specimens and a consistent sampling methodology across  
122 space and time to avoid sample bias (Hao et al., 2020).

123 In particular, the spatially-explicit prediction of fungal productivity, i.e. mushroom  
124 fruiting patterns, is a key feature of fungal dynamics inasmuch as it is tightly related to  
125 the supply of multiple provisioning, regulating and cultural ecosystem services (Boa,  
126 2004). However, the high correlation between mushroom production and meteorological  
127 conditions among other drivers (Taye et al., 2016; Alday et al., 2017; Collado et al. 2019)  
128 makes the prediction of mushroom production challenging, especially in Mediterranean  
129 ecosystems where there is a high inter-annual variability of climatic conditions. The long  
130 period of potential fruiting of different mushroom species, as a result of their adaptation  
131 to the recurrent climatic patterns of a dry summer followed by a wet autumn (Barnard et  
132 al., 2015), makes mushroom yields dependent on a large number of variables.  
133 Precipitation and temperatures on a weekly scale can be the factors that lengthen, shorten  
134 or shift the fruiting period (Gange et al., 2007; Kauserud et al., 2008; Kauserud et al.,  
135 2009; Büntgen et al., 2012), and also those that modulate mushroom production to a  
136 higher degree (Karavani et al., 2018). The large number of variables involved and their  
137 presumed interactions may often yield a misconception that fungal productivity is highly  
138 stochastic or very difficult to predict. Previous research to estimate mushroom  
139 productivity over large scales has been mainly based on mixed-effects modelling (de-  
140 Miguel et al., 2014; Sánchez-González et al., 2019). Despite being a valid approach, it

141 may have certain limitations that are worth assessing in comparison with alternative  
142 methods that remain unexplored.

143 This study compares different statistical and machine learning models in estimating  
144 mushroom productivity at the landscape level, together with a systematic methodology to  
145 determine the best approach to predict mushroom production in forest ecosystems. Using  
146 climatic and biophysical data together with in situ fungal records collected weekly over  
147 more than 20 years on a hundred permanent plots, we developed spatially explicit, high-  
148 resolution continuous maps of mushroom productivity that were also used in the selection  
149 of the most suitable methods for predicting this ephemeral and important forest resource.  
150 We tested six most widely used predictive models to date, namely, generalized linear  
151 mixed-effects models (GLMM), and compared them with geographically weighted  
152 regression models (GWR), as well as with alternative state-of-the-art machine learning  
153 algorithms such as random forest (RF), extreme gradient boosting (XGB), support vector  
154 machine (SVM) and deep learning (DL) models.

## 155 **2 Methods**

### 156 2.1 Study area and sampling plots

157 The study area was Catalonia region, northeastern Spain, in the western Mediterranean  
158 basin. The forest ecosystem types considered in this study were the main Mediterranean  
159 pine forest ecosystems that represent the majority of the forest area of the study region,  
160 namely, pure stands of *Pinus halepensis*, *P. sylvestris*, *P. pinaster*, *P. nigra* and *P. uncinata*  
161 and mixed stands of *P. halepensis* and *P. nigra*, and of *P. sylvestris* and *P. nigra*. We used  
162 a dataset that gathered information from 98 permanent monitoring plots for fungal  
163 dynamics sampled on a weekly basis during the main mushroom fruiting period, between  
164 August and the end of December and from 1997 to 2019. The plots were distributed

165 randomly and proportionally to the relative surface of the different pine forest ecosystems  
 166 (Bonet et al., 2010) (Figure S1). Data were aggregated to an annual basis to create  
 167 predictive models to estimate annual mushroom productivity. More information about the  
 168 sampling methods and data can be found in Bonet et al. (2004), Martínez de Aragón et al.  
 169 (2007) and Table 1.

170 Table 1. Summary of mushroom, climate and physical data of the 98 sampled plots.

	Min.	1 <sup>st</sup> quart.	Median	Mean	3 <sup>rd</sup> quart.	Max.
Mushroom yield (kg ha <sup>-1</sup> year <sup>-1</sup> )	0.00	9.14	47.62	104.46	138.97	1345.78
Slope (degrees)	3.00	12.00	18.00	18.07	23.00	37.00
Aspect (degrees)	4.00	58.00	179.00	166.50	282.00	360.00
August precipitation (mm)	0.00	14.56	29.07	42.10	62.10	170.89
September precipitation (mm)	0.21	37.59	54.94	59.01	77.51	202.79
October precipitation (mm)	4.62	32.50	56.08	73.46	90.13	254.23
August mean temperature (°C)	14.62	20.03	22.71	22.05	24.20	27.31
September mean temperature (°C)	9.47	16.10	18.39	17.86	20.02	23.74
October mean temperature (°C)	7.24	12.36	14.15	13.81	15.58	19.19
August max. temperature (°C)	17.93	25.08	28.34	28.12	30.27	39.26
September max. temperature (°C)	13.61	21.04	23.48	23.43	25.84	33.24
October max. temperature (°C)	10.98	16.77	18.76	19.03	20.84	29.05
August min. temperature (°C)	0.93	11.95	14.36	13.27	15.87	19.04
September min. temperature (°C)	-1.19	8.50	10.77	9.86	12.33	17.29
October min. temperature (°C)	-6.80	4.95	7.46	6.24	8.83	13.50

171

172

## 173 2.2 Climate and biophysical data

174 Meteorological data for each sampling plot was obtained from the interpolation and  
175 altitudinal correction of daily weather of 201 meteorological stations from the Catalan  
176 Meteorological Service and the Spanish Meteorological Agency. Interpolation was  
177 conducted with “meteoland” R package (De Cáceres et al., 2018) that uses a modification  
178 of the DAYMET methodology (Thornton et al., 1997; Thornton and Running, 1999).  
179 Likewise, to determine the typical climatic conditions across the whole study region, we  
180 used the mean of the interpolated daily weather variables for the period between 1991  
181 and 2016 with 1-km resolution. We computed the accumulated monthly rainfall from  
182 August to October and the mean, maximum and minimum monthly temperatures for the  
183 same period, coinciding with the main mushroom fruiting period.

184 The total area covered by the different pine forest ecosystems was retrieved from the  
185 CORINE habitats map (Commission of the European Community, 1991). The  
186 biophysical variables such as elevation, slope, aspect and stand basal area were obtained  
187 at 20-m resolution from the first cover of the LIDARCAT Project  
188 ([http://territori.gencat.cat/es/detalls/Article/Mapes\\_variables\\_biofisiques\\_arbrat](http://territori.gencat.cat/es/detalls/Article/Mapes_variables_biofisiques_arbrat)) based  
189 on different LiDAR flights between 2008 and 2011 with a point density of 0.5 points/m<sup>2</sup>.

## 190 2.3 Analytical methods

191 We used and compared six different analytical methods to predict annual mushroom  
192 productivity. Two analytical approaches were based on statistical methods, namely,  
193 generalized linear mixed-effects models (GLMM) and geographically weighted  
194 regression (GWR), whereas the other four analytical methods were based on alternative  
195 machine learning approaches, namely, random forest (RF), extreme gradient boosting  
196 (XGB), support vector machine (SVM) and deep learning (DL).

197 2.3.1 Statistical modelling

198 We used a two-stage modelling approach to take into account the high frequency of  
199 “zero” production values in many sample plots over time (Hamilton and Brickell, 1983;  
200 de-Miguel et al., 2014; Karavani et al., 2018; Collado et al., 2018). The high occurrence  
201 of these values arise from the small size of the plots and the stochastic nature of  
202 mushroom emergence (de-Miguel et al., 2014).

203 The first stage determines the probability of mushroom emergence, according to binomial  
204 data of presence/absence, using a logistic regression  $\pi(X)=E(Y|X)$  and a logit link  
205 function to represent the conditioned mean of Y given X (Eq. 1 and 2).

$$206 \quad \pi(x_k) = E(Y|x_k) = \frac{1}{1+e^{-g(x_k)}} \quad (1)$$

$$207 \quad g(x_k) = \ln\left(\frac{\pi(x_k)}{1-\pi(x_k)}\right) = \beta_0 + \beta_k x_k \quad (2)$$

208 where  $\pi(x_k)$  is the probability of mushroom occurrence,  $g(x_k)$  the logit transformation of  
209  $\pi(x_k)$ ,  $Y$  is the dependent variable (mushroom presence/absence),  $x_k$  is  $k^{\text{th}}$  independent  
210 variable,  $\beta_0$  is the intercept parameter and  $\beta_k$  is the regression coefficient for  $k^{\text{th}}$   
211 independent variable.

212 The second stage was based on the modelling of the production of non-zero production  
213 values at logarithmic scale using linear regression  $y=E(\log(Y)|X) + \varepsilon$ . Logarithmic  
214 transformation allows to limit the production range in the interval  $[0, \infty)$ , depending on  
215 the values of X (Eq. 3). The proportional bias of the logarithmic regression was corrected  
216 with the Snowdon’s bias correction factor (Snowdon, 1991) based on the ratio of the  
217 arithmetic sample mean and the mean of the back-transformed predicted values from the  
218 regression (Eq. 4):

$$219 \quad \ln(\text{prod}) = \beta_0 + \beta_k x_k + \varepsilon \quad (3)$$

220  $CF = Y/\hat{y}$  (4)

221 where  $\ln(prod)$  represents the non-zero production of mushrooms at logarithmic scale,  $\beta_0$   
222 is the intercept parameter,  $\beta_k$  the regression coefficient for  $k^{th}$  independent variable,  $\varepsilon$  the  
223 random error of the deviation of the observations from the conditioned mean of  $\ln(Y)$  and  
224  $Y/\hat{y}$  is the ratio between the mean of observed and the mean of predicted values of the  
225 sapling units.

226 Finally, the total production of mushrooms was obtained from the product of the  
227 probability of appearance and the conditioned production of non-zero values (Eq. 5).

228  $yield = \pi(x_k) e^{\ln(yield)} CF$  (5)

229 where  $\pi(x_k)$  is the probability of mushroom occurrence,  $\ln(yield)$  represents the production  
230 of mushrooms at logarithmic scale and  $CF$  is bias correction factor.

### 231 2.3.1.1 Generalized Linear Mixed Models

232 Due to mushrooms sampling methodology, where annually data was taken from a  
233 network of permanent plots, we used Generalized Linear Mixed Models GLMM (de-  
234 Miguel et al., 2014; Karavani et al., 2018; Collado et al., 2018). This method can consider  
235 the spatial and temporal autocorrelation among observations (Pinheiro and Bates, 2000)  
236 adding random effects to segment the data into different groups according to year and  
237 plot. In the proposed mixed-effects models only random effects on model interception  
238 were considered. All the models were fitted using the “glmer” function from the “lme4”  
239 R package (Bates et al., 2014).

### 240 2.3.1.2 Geographically Weighted Regression

241 GWR is a non-stationary modelling technique that describes the spatially varying  
242 relationships between the dependent variable and the explanatory variables (Páez and

243 Wheeler, 2009). Coefficients of a GWR-based model are given by the spatial location of  
244 data and can be estimated for any new location. This means that given a grid, the estimated  
245 coefficients for each point in space vary continuously as a function of the spatial  
246 heterogeneity of the relationships.

247 Coefficients for each regression point were calibrated using the data around itself. Due to  
248 the annual sampling methodology and the geographical distribution of plots, some plots  
249 were grouped denser in some areas and less dense in others. Consequently, we used an  
250 adaptive window according to the spatial density of our plots (Georganos et al., 2017).  
251 Occurrence and conditional production models, as well as the optimal data value for  
252 adjusting the adaptive window, were obtained from the "ggwr" and "gwr.set" functions,  
253 respectively, of the R package "spgwr" (Bivand et al., 2014).

## 254 2.3.2 Machine learning modelling

### 255 2.3.2.1 Decision trees-based models (random forest and extreme gradient boosting)

256 RF algorithm (Breiman, 2001) is based on an ensemble learning method that detects  
257 general patterns present in observed data using a defined number of decision trees. Trees  
258 are grown independently of each other, achieving less correlation between them. This is  
259 achieved by selecting a random subset of the predictors, in each node, to be chosen as the  
260 best candidate for use in each of the divisions (Breiman, 2001).

261 The hyperparameters that we tuned in the RF models were the number of trees and the  
262 optimal number of predictor candidates to be chosen in each node. The first one was tuned  
263 by training a sequence of models with 1 tree and up to 500, other things being equal, to  
264 locate the minimum number of trees required to minimize the prediction error. Once this  
265 value was set, we evaluated the optimal number of predictor candidates to be chosen in  
266 each node in a similar way, picking the one that minimizes the error while growing less

267 correlated forests. In both cases, cross-validation was used (randomly splitting 95% of  
268 the data for training and the remaining 5% for validation) and 20 models were trained for  
269 each combination of hyperparameters (Table S3). Hyperparameters tuning and model  
270 training were done with the R-package “RandomForest” (Liaw and Wiener, 2002).

271 Unlike RF, the technique of gradient boosting (Friedman, 1999) does not create each  
272 decision tree independent of each other, but rather the trees are built sequentially. Thus,  
273 each constructed tree uses the information on the previously cultivated trees (Jamet et al.,  
274 2013). XGB is a specific implementation of the boosting method that allows finding the  
275 best tree by minimizing the loss function using a minimum amount of resources (Chen  
276 and Guestrin, 2016). To minimize model overfitting, XGB is basically based on two  
277 techniques: shrinkage and column subsampling. This means that, in each iteration, a  
278 fraction of the observed data is used to grow the next tree, using the weighted information  
279 from each of the previous trees.

280 As in RF-hyperparameters tuning, we used cross-validation by training 20 models for  
281 each hyperparameters combination. We tuned the number of iterations, in a range  
282 between 1 and 100, according to the learning rate (eta) to improve the prediction accuracy  
283 and optimize the XGB algorithm. Next, we tuned the depth of the model trees and finally,  
284 since this depends on the others, the gamma regularization parameter to avoid model  
285 overfitting (Table S4). The R-package "xgboost" (Chen and He, 2020) was used here to  
286 train the XGB models and tune their hyperparameters.

#### 287 2.3.2.2 Support Vector Machine

288 SVM (Cortes and Vapnik, 1995) was created to solve classification problems by adjusting  
289 a hyperplane that delimited the different categories while minimizing the distance  
290 between the hyperplane and the closest points. Although its main purpose was to be used

291 in classification problems, later updates have made this algorithm applicable to regression  
292 tasks, using the same principles with which it was conceived. In the case of regression, a  
293 tolerance margin is established, corresponding to the support vectors, and an appropriate  
294 hyperplane is defined to adjust the data.

295 A radial-based kernel function was used both to train the SVM models and to select their  
296 optimal hyperparameters. The cost and gamma hyperparameters were tuned to each other  
297 based on a cross validation of the predictions made by 20 models, with values between 1  
298 and 50 and between 0.1 and 0.9, respectively (Tale S5). SVM models and their hyper-  
299 parameter tuning were done using the R-package "e1071" (Meyer et al., 2019).

### 300 2.3.2.3 Deep Learning

301 Machine learning includes those algorithms that generate models from patterns in a data  
302 set, making it interesting for the analysis of complex and non-linear data (Olden et al.,  
303 2008). While other machine learning algorithms find patterns among the variables used  
304 to train the models, DL is able to detect and extract undescribed characteristics directly  
305 among the highly dimensioned data (Christin et al., 2019). These characteristics have led  
306 to an increase in the use of these algorithms in recent years in ecology (Christin et al.,  
307 2019).

308 As in the tuning of the best hyperparameters for each of the others machine learning  
309 model, we proposed different candidate structures, given by the following set of  
310 hyperparameters, for the DL models network. We trained models with 1, 2 and 3 hidden  
311 layers with a "relu" regularization function and a final layer with a single node and the  
312 same regularization function. For each structure, we used hidden layers with 8, 16, 32, 64  
313 and 128 nodes in each one. To reduce overfitting, we randomly dropped out (setting to  
314 zero) 50% of output features of the layer during training. We evaluated each structure

315 from the cross-validation of the predictions of 20 models to minimize the prediction error  
316 (Table S6). We used the R-package "keras" (Allaire and Chollet, 2019) to train the final  
317 DL models and the different proposed structures.

### 318 2.3.3 Model and variable selection and evaluation

319 Statistical model evaluation and variable selection was based on the current knowledge  
320 of forests and mushroom ecology, the statistical significance of model parameters  
321 ( $p < 0.05$  or  $t > |1.96|$ ), the variance inflation factor (VIF) to quantify the severity of  
322 multicollinearity and the parsimony principle. To check the sensitivity/specificity of the  
323 binomial classification models we used Receiver Operator Characteristic (ROC) curves,  
324 using the R package "ROCR" (Sing et al., 2005).

325 To assess whether GWR improved GLMM due to the non-stationary nature of data and  
326 to avoid introducing an improvement that was not attributed to the type of modelling, the  
327 same explanatory variables as in GLMM were used. To test the non-stationarity of the  
328 independent variables of GWR models, the local parameters were compared with global  
329 GLMM coefficients. The probability of incorporating non-stationary variables increases  
330 if the estimated coefficient of the variable in GLMM ( $\pm$  standard error) is outside the 1<sup>st</sup>  
331 and 3<sup>rd</sup> quartile of the GWR model coefficient (Propastin, 2009).

332 For each of the four machine learning algorithms, two types of models were adjusted. The  
333 first ones were trained using a total of 15 biophysical variables (Table 1), while the second  
334 ones were trained using a subset of them. This subset was determined from the same 5  
335 variables used in the statistical models, including climate predictors only. This allowed  
336 us to assess separately the prediction accuracy due to the analytical method, and the  
337 prediction accuracy due to differences between predictors or the number of explanatory  
338 variables.

339 Due to the randomness in the training stage of RF and XGB algorithms, and for  
340 consistency with the methodology used for SVM and DL models, 50 models were trained  
341 from 50 bootstrapping iterations, selecting randomly 95% of the data.

342 In machine learning-based approaches, the relationship between predictors and  
343 mushroom productivity was assessed based on partial dependence plots (PDPs), a low-  
344 dimensional graphical rendering between variable pairs, in order to determine whether  
345 this relationship lacked ecological sense (within a set of specific predictors, and in this  
346 particular case, corresponding to the training data set).

#### 347 2.3.4 Evaluation of the predictive performance and mapping

348 Since the main purpose of this study was to develop models to accurately predict  
349 mushroom productivity, this entails the evaluation of the predictive performance of the  
350 resulting models also outside of the range of the training (or fitting) region. With the aim  
351 of determining the similarities between sampled plots and the territory where it was used  
352 to estimate the mushroom yield, a principal component analysis (PCA) based on the  
353 models' predictors was used. In addition, to evaluate and compare the predictive accuracy  
354 of the models, different cross-validation strategies were used (Roberts et al., 2017). This  
355 validation was done by comparing the determination coefficient ( $R^2$ ), root mean squared  
356 error (RMSE) and mean absolute error (MAE) of observed (using 95% of the data) against  
357 predicted (i.e. the remaining 5% of the data) values of each model using 50 bootstrapping  
358 iterations. To inspect in depth, the source of the errors in the models, the mean square  
359 deviation (MSD) was estimated and also decomposed in additive components, namely,  
360 squared bias (SB), nonunity slope (NU) and lack of correlation (LC) (Gauch et al., 2003).  
361 The alternative cross-validation strategies utilized were:

362 i. Substitution: the testing data was part of the same training data

363 ii. Random: the training and testing data set were selected randomly

364 iii. Spatial blocking: to avoid underestimating the prediction error due to the spatial  
365 structure of the data the training and testing data were strategically and non-randomly  
366 selected (Roberts et al., 2017). The two data sets were selected in different geographical  
367 areas, selecting a randomly plot and blocking the closest plots as testing data.

368 iv. Climate blocking: since plots were spatially distributed among different bioclimatic  
369 areas, we conducted an environmental blocking (Valavi et al., 2018) considering the  
370 differences in climatic conditions between plots. Similar to spatial blocking (Roberts et  
371 al., 2017), we used the two-dimensional space described by the first two PCA components  
372 (based on the sets of five and twelve climatic model predictors, respectively) to select the  
373 training and testing datasets from different climatic areas. In this 2-D space, one plot was  
374 randomly selected and blocked as testing data together with a given number of  
375 neighbouring plots.

376 A 10% and 20% blocking was also considered to determine the error in climatic and  
377 geographical areas more different from the sampled data (as a comparison it was also  
378 done in the random blocking), providing a more differentiated dataset of training and  
379 testing.

380 To generate the landscape-level mushroom productivity maps based on RF, XGB, SVM  
381 and DL, we used the mean estimation of the 50 trained models. Otherwise, estimates from  
382 statistical models were the result of the empirical model predictions, fitted with 100% of  
383 data. These maps were constructed with a resolution of 1 km in accordance with the  
384 resolution of the climatic data. As a result of the estimates of the 50 models, spatially  
385 explicit relative standard error (SE) maps were also created for each methodology.

386 The final maps were evaluated on the basis of knowledge about fruiting patterns, and also  
387 on whether they followed ecologically logical patterns (related to climatic conditions).  
388 Therefore, we would expect smoothed estimates across the territory and conditioned by  
389 the variations of those most important variables in each model.

### 390 **3 Results**

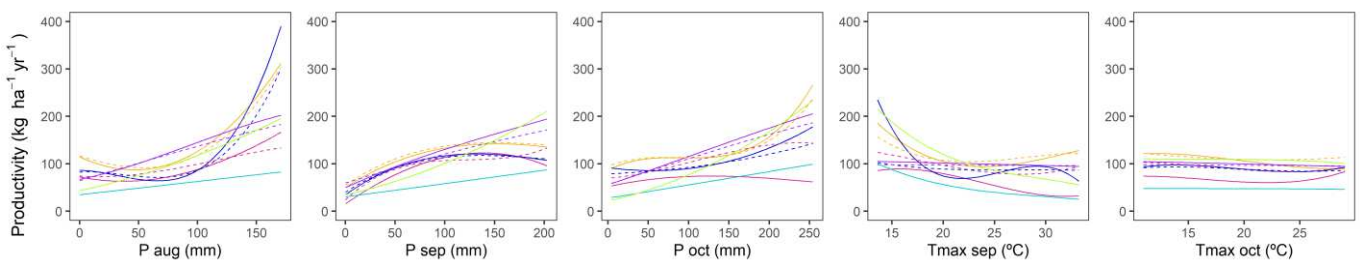
#### 391 3.1 Relationships between dependent and explanatory variables

392 Statistical models showed a statistically significant and positive relationship of mushroom  
393 productivity with rainfall in August, September and October (both in conditioned  
394 production and occurrence models). On the other hand, conditioned production and  
395 occurrence models also showed a statistically significant and negative relationship with  
396 the maximum temperature of August and October, respectively (Tables S1 to S3). Yet,  
397 the coefficients of GWR models varied according to geographical location (Table S3 and  
398 Figure S2), describing certain non-stationarity in both precipitation and temperature.

399 Within GLMM models, PDPs showed an almost linear relationship between the amount  
400 of precipitation between August and October and mushroom productivity in the model fit  
401 data range. In contrast, GWR showed an accelerated growth in productivity by increasing  
402 rainfall, which was accentuated in those locations with a higher precipitation regression  
403 coefficient. Besides, and similarly in GLMM and GWR, the maximum temperature in  
404 August showed a decelerated decrease in productivity by increasing temperature, while  
405 the maximum temperature of October, even though it showed a negative relation, resulted  
406 in little relevance in mushroom productivity for the range of values of the fitting data  
407 (Figure 1).

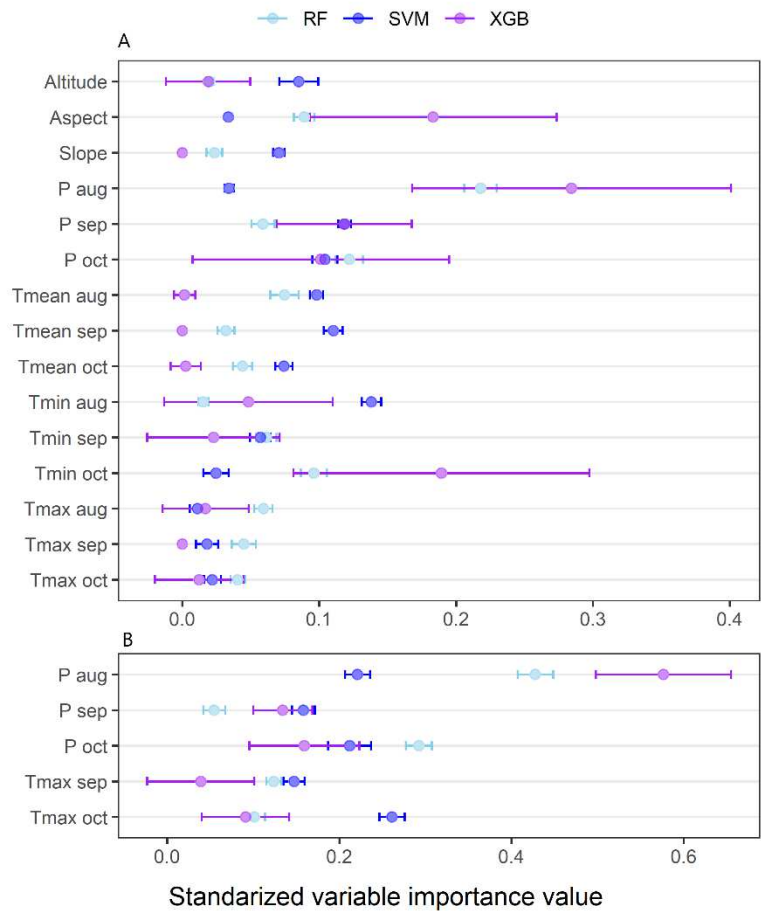
408 Different machine learning models resulted in rather similar relationships between  
409 variables although, due to the particularities of each algorithm, the patterns changed

410 slightly between approaches. In contrast to the relationships in GLMM and GWR models,  
 411 some of the machine learning models did not show monotonically increasing or  
 412 decreasing relationships between dependent and explanatory variables. This monotony  
 413 was often broken at the extremes of the range of values of the predictor variables, where  
 414 the amount of data to train the models was lower (Figure 1). Moreover, machine learning  
 415 methods also showed differences in the importance assigned to different predictors. Thus,  
 416 XGB identified some variables as very important compared to other predictors.  
 417 Specifically, in the models trained with 15 variables, XGB showed a greater importance  
 418 of precipitation in August, September and October, minimum temperature in October and  
 419 aspect. In addition, precipitation of August resulted in having further greater importance  
 420 in the models trained with 5 variables. Conversely, the importance detected by RF and  
 421 SVM to the whole array of predictors was more homogeneous. RF showed a greater  
 422 importance to the same variables as XGB, while the most important variables in SVM  
 423 were precipitation in September and October, average temperature in August and  
 424 September, and minimum temperature in August (Figure 2).



425 Figure 1. Relationship between annual mushroom productivity and August, September  
 426 and October precipitation and maximum temperatures in September and October (these  
 427 variables are the variables used in the statistical models and the five variables machine  
 428 learning models). Yellow (random forest), blue (extreme gradient boosting), violet  
 429 (support vector machine), purple (deep learning), light blue (generalized linear mixed  
 430 models) and light green (geographically weighted regression) colours refer to the

431 different modelling techniques. Continuous line includes the models that use the five  
 432 variables and the dashed line the machine learning models trained with 15.



433 Figure 2. Standardized variable importance value used to train random forest (RF),  
 434 extreme gradient boosting (XGB) and support vector machine (SVM) models with 15 (A)  
 435 and 5 (B) variables. Variable importance values represent the contribution of each  
 436 variable to predict the annual mushroom productivity.

437 GLMM and GWR fitted models and their coefficients are shown in the supplementary  
 438 material in Table S1 to S3. Likewise, machine learning hyperparameters can be found in  
 439 the supplementary material in Figure S3 to S6.

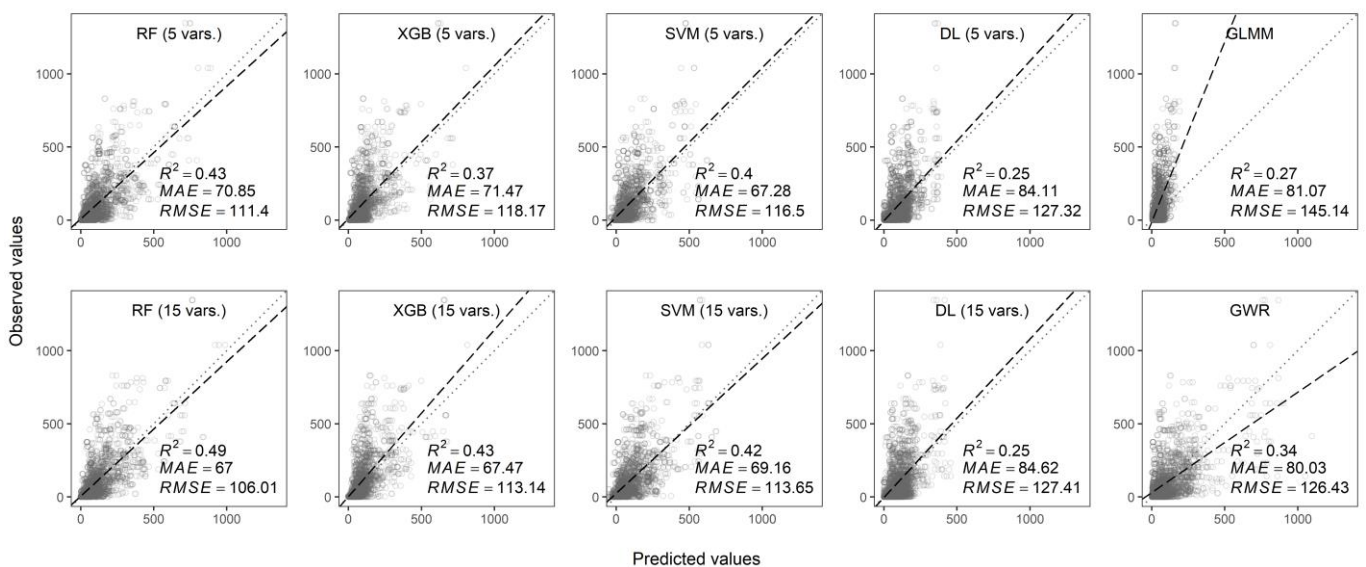
440

441

442

443 3.2 Predictive accuracy of different methods

444 In general, machine learning models showed better predictive accuracy compared to  
 445 statistical models. Above all, models based on decision trees, and more specifically RF,  
 446 stood out as the models with the lowest error. RF, XGB and SVM models trained with 15  
 447 variables showed lower errors than the same ones trained with five variables, while DL  
 448 models resulted in similar prediction error regardless the amount of predictors. Moreover,  
 449 RF trained with five variables resulted in lower or similar error compared to XGB and  
 450 SVM models trained with 15 variables (Figure 3 and Table S4).



451 Figure 3. Cross-validation of estimated total mushroom production ( $\text{kg ha}^{-1} \text{ year}^{-1}$ ) using  
 452 random forest (RF), extreme gradient boosting (XGB), support vector machine (SVM)  
 453 and deep learning (DL) trained with 15 and 5 variables and generalized linear mixed  
 454 models (GLMM) and geographically weighted regression (GWR). Pointed line shows the  
 455 equality line and the dashed one the best fit between predicted and observed values. It  
 456 shows  $R^2$  mean absolute error (MAE), root-mean-squared error (RMSE) and coefficient of  
 457 determination ( $R^2$ ) of the relation for each technique.

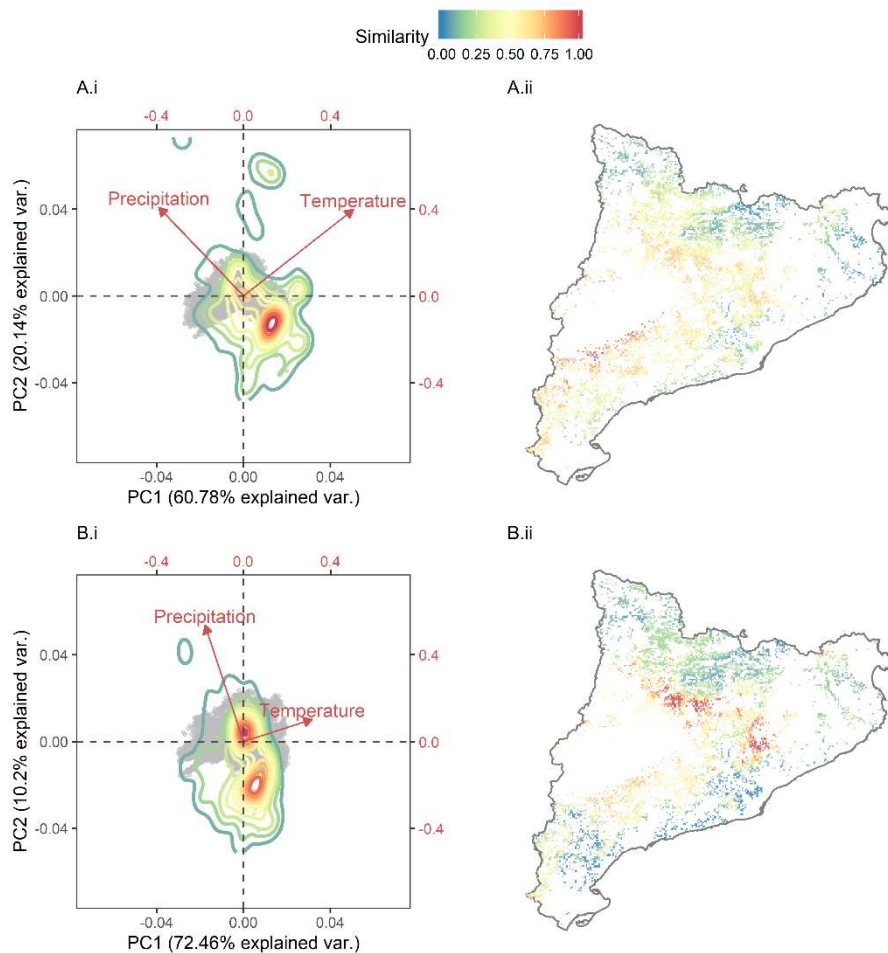
458 The assessment of the predictive performance based on random blocking resulted in lower  
 459 accuracy compared to spatial and climatic blocking in RF, XGB and SVM models. This

460 trend was not so obvious in DL or statistical models. In climate blocking, the prediction  
461 error increased with increasing proportion of blocking data, denoting lower predictive  
462 accuracy of fungal productivity (Table S4) in areas with very different climatic conditions  
463 compared to the training data (Figure 4). Most machine learning models, based on finding  
464 patterns in supplied training data, showed very low errors when making predictions in a  
465 similar environment as the training data (substitution), i.e. approximately 50% and 75%  
466 lower error in RF and XGB, respectively, compared to random blocking. Overall, RF was  
467 the approach with lower error, being lower in models trained with 15 variables than those  
468 trained with five variables (105 and 114 respectively in a random blocking and 110 and  
469 111 in a climate blocking). Compared to the other tested models (in terms of RMSE in  
470 random blocking), RF results in an improvement between 7 and 31% in the models trained  
471 with 15 variables and between 4 and 26% in the RF models trained with 5 variables (Table  
472 S4).

473 Although in all the analytical approaches the main source of the error was due to the  
474 variation between training and testing data (i.e. lack of correlation, LC), the statistical  
475 models also resulted in high NU value, leading to under- or overestimation of annual  
476 mushroom productivity for certain ranges of the data. In GLMM, where the slope of the  
477 best linear fit between observed and predicted values was greater than 1, there was a clear  
478 underestimation. Moreover, GWR showed a slope between 0 and 1, leading to a  
479 production overestimation. On the contrary, machine learning models corrected this  
480 under- or overestimation by reducing the NU value and approximating the slope to 1  
481 (Table S4).

482

483

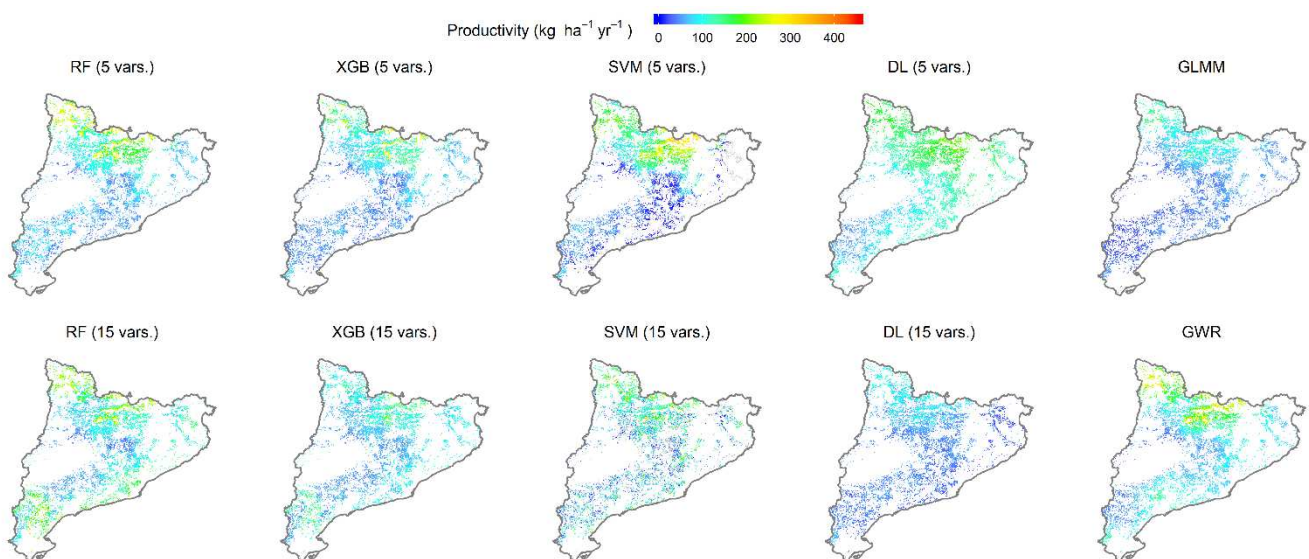


484 Figure 4. Similarity between the annual meteorological data of the sampled plots (used to  
 485 train the models) and the average climatology of the Catalan pine forests (used to predict).  
 486 Graphs show the climatology of the different pixels (grey) that form the map of pine  
 487 forests in Catalonia from a two-dimensional representation based on a principal  
 488 component analysis (PCA). The meteorological characteristics of the registered plots are  
 489 shown from a density map of points within the bivariate space. Within this space, each  
 490 pixel of pine forests matches a value of meteorological records density, being able to  
 491 extrapolate this information to a map of the study region, obtaining a spatially explicit  
 492 map of the similarity between these two datasets. (A.i) (A.ii) correspond to the similarities  
 493 by creating a bivariate space resulting from PCA of 5 climatic variables (which can be  
 494 used for the less dimensioned models), while (B.i) and (B.ii) are based on a PCA of 12  
 495 climate variables (which can be used in the models trained with 15 climatic variables).

496 3.3 Mapping and accuracy of predictions at the landscape level

497 The spatially explicit predictions at the landscape level from each model resulted in rather  
498 similar general patterns (Figure 5). Namely, they predicted higher productivity in the  
499 northern areas of the study region, characterized by higher altitudes, i.e., Pyrenees  
500 mountain range. Also, the different models reproduced similar patterns within these areas  
501 according to variations in local topography. In addition, RF, XGB and SVM models  
502 trained with 15 predictors (not in DL) yielded higher estimates of mushroom productivity  
503 in coastal areas compared to the same algorithms based on a subset of 5 predictors.

504 RF, XGB and SVM trained with 15 variables also resulted in less smoothed predictions  
505 of mushroom yield across the territory compared to estimates based on the subset of 5  
506 predictors. Furthermore, SVM produced illogical predictions below  $0 \text{ kg}\cdot\text{ha}^{-1}\cdot\text{year}^{-1}$  in a  
507 few spatially localized areas when 5 variables were used, and scattered throughout the  
508 territory when using 15 predictors. In contrast, DL resulted in very smoothed estimates  
509 across the territory, contrary to the maps obtained from all the other machine learning  
510 methods (Figure 5).



511 Figure 5. Landscape-level prediction of total annual mushroom productivity, using  
512 random forest (RF), extreme gradient boosting (XGB), support vector machine (SVM)

513 and deep learning (DL) trained with 15 and 5 variables, respectively, and generalized  
514 linear mixed models (GLMM) and geographically weighted regression (GWR) fitted  
515 using 5 predictors.

516 In addition, the mushroom productivity predictions based on RF, XGB, SVM and GWR  
517 ranged between 0, in the less productive areas, and approximately 300 and 400 kg·ha<sup>-1</sup>  
518 ·year<sup>-1</sup>. Slightly lower productivity was detected using GLMM and DL for the most  
519 productive sites, i.e. not exceeding 200 kg·ha<sup>-1</sup>·year<sup>-1</sup> in any point of the study area.

520 ML models trained with 5 variables resulted in rather low relative SE in practically all  
521 the study area, whereas the models based on 15 predictors resulted in high relative SE in  
522 the coastal areas, i.e. those areas with the most different bioclimatic conditions compared  
523 to the training data. Finally, predictions using DL with 15 variables showed a high relative  
524 SE throughout the whole territory (Figure S7).

#### 525 **4 Discussion**

526 To our knowledge, this is the first study addressing a systematic evaluation of the  
527 predictive performance of alternative statistical and machine learning models to predict  
528 mushroom productivity, and one of the few systematic comparisons between these  
529 different predictive approaches within the field of ecological research. This was  
530 conducted using one of the largest datasets (if not the largest one) for fungal productivity  
531 monitoring, based on consistent sampling methodology and taxonomic identification of  
532 mushrooms over more than 20 years on nearly a hundred permanent sampling plots,  
533 randomly distributed throughout the study region, which contributes to overcoming most  
534 of the practical problems related to the existence of available data for modelling fungal  
535 resources (Hao et al., 2020).

536 When dealing with complex ecological interactions between multiple potential  
537 explanatory variables, our results show that statistical models, specially GLMM, clearly  
538 seem to have lower predictive performance compared to artificial intelligence-based  
539 approaches, in line with previous research (e.g. Smoliński and Radtke (2016) and Schratz  
540 et al. (2019)). They were less accurate and produced large over- or underestimation of  
541 mushroom productivity, making them unreliable for such purposes compared to other  
542 alternatives. On the other hand, statistical models can be good candidates for detecting  
543 the most appropriate variables to be used in machine learning models and unravel  
544 environmental-ecological relationships between them (Shmueli, 2010; Schratz et al.,  
545 2019), since the inherent statistical assumptions that shape these models allow the  
546 relationships between data in a set of probability distributions to be correctly  
547 approximated. However, adding a spatial factor to the statistical models was able to  
548 correct for the strong underestimation of GLMM in high productivity values. By  
549 considering a spatial component, we were able to find stationary patterns in the predictors,  
550 denoting that climatic conditions do not affect equally across the study area.

551 As demonstrated here, choosing a subset of variables from statistically significant  
552 predictors in statistical models can help us to deal with some drawbacks. A problem with  
553 selecting a single subset of variables from a machine learning models is that, due to the  
554 algorithm itself, the significance is adjusted differently and could be inappropriate for  
555 some of them. For example, within decision tree algorithms, XGB determines the variable  
556 to be used in each node of the tree among the total of variables of a model, while RF does  
557 it within a subset of them, giving greater probability of being chosen to those less  
558 important variables (Hastie et al., 2001). On the other hand, and depending on the  
559 relationship between variables, the importance of a set of correlated variables can be  
560 distributed among the different predictors (giving lower importance to each one of them),

561 but the total importance that this set represents in the predictive performance is  
562 remarkable (Toloşi and Lengauer, 2011). This can cause that when discarding the less  
563 important variables, this set of predictors is omitted, causing a notorious drop in predictive  
564 performance. Moreover, in a group of correlated variables where there is only one true  
565 predictor (the one that implies real causality), machine learning algorithms could give  
566 similar values of importance to the whole set of variables (Archer and Kime, 2007),  
567 actually hiding the true predictor. Consequently, each machine learning algorithm give a  
568 different importance to each variable. Therefore, to identify the variables that could best  
569 explain the processes that occur in natural ecosystems and/or use the variable importance  
570 to select a subset of predictors to train a more parsimonious model, the above  
571 considerations should be taken into account.

572 Based on the prediction error of different models, it would seem logical to think that  
573 models trained with 15 variables are better at achieving the goal of predicting mushroom  
574 productivity (they have lower predictive error) compared to models based on five  
575 predictors. However, they have some remarkable drawbacks. Using a larger amount of  
576 variables one can account for more information about potential environmental drivers.  
577 This might seem useful, because such information can help to improve predictions in  
578 specific cases. However, using a larger number of variables also increases exponentially  
579 the dimensions of the ecosystem space, commonly known as curse of dimensionality  
580 Hughes (1968), which makes it more difficult to match the ranges of the modelling data  
581 in extrapolation to a broader study area. In addition, not taking into account the data  
582 spatial dependencies may increase the likelihood of getting out-of-bag misinterpretations  
583 with increasing number of predictor variables (Meyer et al., 2018, 2019a). Conversely,  
584 using fewer variables results in higher similarity (in terms of climatic conditions) between  
585 the training and testing data. In particular, by creating a 2-D space based on PCA using

586 five climatic variables, the entire prediction zone was practically similar to the training  
587 data, while by using twelve climatic variables it decreases considerably (Figure 4).  
588 Compared to other alternative environmental blocking approaches (Valavi et al., 2018),  
589 our climatic blocking approach allowed us to identify the similarity between training and  
590 testing data as well as select the same amount of data in each blocking strategy. Assuming  
591 that spatial or climatic blocking are proper approaches to estimate the error in  
592 geographically (Roberts et al., 2017; Meyer et al., 2019a) or climatically different areas,  
593 and random blocking informs about the error in similar areas, we can determine which  
594 strategy will be best in each case. Knowing this, we can expect that random blocking may  
595 be more informative of the error of mushroom productivity estimates made by 5-variable  
596 models. On the other hand, in the spatial or climatic blockade it may be more correct to  
597 estimate the error of the estimates made by 15-variable models. In this way we can see  
598 that, in those areas where the error of the estimates of the 15-variable models is given by  
599 the spatial block and in the 5-variable models by the random block, a lower error is  
600 achieved with the second set of models. This is evident throughout the coastal zone of the  
601 study area and in the higher parts of the Pyrenees mountain range, where the error will be  
602 lower when using models with a smaller number of variables. Thus, it seems that  
603 parsimony can be useful model selection criterion not only for statistical methods, but  
604 also for machine learning algorithms (Coelho et al., 2018).

605 As noted, statistical models do not seem to be competitive compared to machine learning  
606 approaches due to poor predictive performance. Among the machine learning models, the  
607 DL approach had the highest prediction error and also resulted in biogeographic patterns  
608 that did not seem to agree with the expected climatic variations throughout the study area.  
609 In turn, SVM yielded illogical negative values of mushroom productivity in some areas.  
610 Therefore, the best candidate methods are the decision trees-based algorithms, i.e. RF and

611 XGB. Between both approaches, RF is preferable since it fits very well for this type of  
612 predictions, where the error mostly arises from the high variability of the studied  
613 ecological item (Hastie et al., 2001). This results in RF having the lowest error in all  
614 criteria analysed (Table S4), being better at estimating in sampling-like environments as  
615 in extrapolation. By estimating a value from the mean between the values given by a set  
616 of trees that are little, or not, correlated between them, it allows to reduce the variance.  
617 This study shows that, although machine learning algorithms allow, due to their  
618 characteristics, to fit models using a large number of variables, it may be advisable to  
619 make a selection of predictors to reduce the multidimensional space defined by the data  
620 to be predicted and thus become more similar to training data. This does not only allow  
621 us to address the selection of the best modelling approach to predict mushroom  
622 productivity; it also provides a methodology, due to the current paucity of data to build  
623 process-based models (Hao et al., 2020), that can be reasonably used in extrapolation out  
624 of the range of the modelling data. This is especially relevant in a context of global  
625 change, where climatic conditions are predicted to change over the years beyond the  
626 historical climatic ranges.

627

628

629

630

631

632

633

634 **List of abbreviations**

635 DL: Deep Learning

636 GLMM: Generalized Linear Mixed Models

637 GWR: Geographically Weighted Regression

638 MAE: Mean Absolute Error

639 PCA: Principal Component Analysis

640 PDP: Partial Dependence Plots

641 RF: Random Forest

642 RMSE: Root Mean Squared Error

643 SE: Standard Error

644 SVM: Support Vector Machine

645 XGB: Extreme Gradient Boosting

646

647

648

649

650

651

652

653

654 **Author's contributions**

655 JMdA, JAB and SdM contributed in the installation of the sampling plots and data  
656 collection. AM, SdM and JL analysed the data. AM wrote the manuscript. All authors  
657 participated in the review and editing of the manuscript. SdM supervised the work during  
658 the whole process.

659 **Funding**

660 This work was supported by the Secretariat for Universities and of the Ministry of  
661 Business and Knowledge of the Government of Catalonia and the European Social Fund.  
662 This work was partially supported by the Spanish Ministry of Science, Innovation and  
663 Universities, grant RTI2018-099315-A-I00. J.A.B. benefitted from a Serra-Hünter  
664 Fellowship provided by the Government of Catalonia.

665 **Acknowledgements**

666 Not applicable.

667 **Availability of data and material**

668 The datasets generated and/or analyzed during the current study are not publicly available  
669 due to legal constraints because they are owned by different institutions, but are available  
670 from the authors on reasonable request.

671 **Ethics declarations**

672 Ethics approval and consent to participate: Not applicable.

673 Consent for publication: Not applicable.

674 Competing interests: The authors declare that they have no competing interests.

675

676 **References**

- 677 Alday JG, Martínez de Aragón J, de-Miguel S, Bonet JA (2017) Mushroom biomass and  
678 diversity are driven by different spatio-temporal scales along Mediterranean  
679 elevation gradients. *Scientific Reports*, 7(1). doi:10.1038/srep45824
- 680 Allaire, JJ, Chollet, F (2019) keras: R Interface to 'Keras'. R package version 2.2.5.0.  
681 <https://CRAN.R-project.org/package=keras>
- 682 Archer KJ, Kimes RV (2008) Empirical characterization of random forest variable  
683 importance measures. *Computational Statistics & Data Analysis*, 52(4), 2249–2260.  
684 doi:10.1016/j.csda.2007.08.015
- 685 Bahn V, McGill BJ (2012) Testing the predictive performance of distribution models.  
686 *Oikos*, 122(3), 321–331. doi:10.1111/j.1600-0706.2012.00299.x
- 687 Barnard RL, Osborne CA, Firestone MK (2014) Changing precipitation pattern alters soil  
688 microbial community response to wet-up under a Mediterranean-type climate. *The*  
689 *ISME Journal*, 9(4), 946–957. doi:10.1038/ismej.2014.192
- 690 Bastin J-F, Finegold Y, Garcia C, Mollicone D, Rezende M, Routh D, Constantin MZ,  
691 Crowther TW (2019) The global tree restoration potential. *Science*, 365(6448), 76–  
692 79. doi:10.1126/science.aax0848
- 693 Bates D, Mächler M, Bolker B, Walker S (2015) Fitting Linear Mixed-Effects Models  
694 Using lme4. *Journal of Statistical Software*, 67(1), 1-48. doi:10.18637/jss.v067.i01
- 695 Bivand R, Yu D (2017) spgwr: Geographically Weighted Regression. R package version  
696 0.6-32. <https://CRAN.R-project.org/package=spgwr>

- 697 Boa E. (2004) Wild edible fungi: a global overview of their use and importance to people.  
698 Non-Wood Forest Products, No. 17, FAO. Forestry Department, Rome, Italy, 148p.  
699 ISBN: 92-5-105157-7
- 700 Bonet JA, Fischer CR, Colinas C (2004) The relationship between forest age and aspect  
701 on the production of sporocarps of ectomycorrhizal fungi in *Pinus sylvestris* forests  
702 of the central Pyrenees. *Forest Ecology and Management*, 203(1-3), 157–175.  
703 doi:10.1016/j.foreco.2004.07.063
- 704 Bonet JA, Palahí M, Colinas C, Pukkala T, Fischer CR, Miina J, Martínez de Aragón, J  
705 (2010) Modelling the production and species richness of wild mushrooms in pine  
706 forests of the Central Pyrenees in northeastern Spain. *Canadian Journal of Forest  
707 Research*, 40(2), 347–356. doi:10.1139/x09-198
- 708 Bonete IP, Arce JE, Figueiredo Filho A, Retslaff FA de S, Lansanova LR (2020)  
709 Artificial neural networks and mixed-effects modeling to describe the stem profile of  
710 *Pinus taeda* l. *floresta*, 50(1), 1123. doi:10.5380/ufv.v50i1.61764
- 711 Breiman L (2001) Random Forest. *Machine Learning*, 45(1), 5–32.  
712 doi:10.1023/a:1010933404324
- 713 Büntgen U, Kauserud H, Egli S (2012) Linking climate variability to mushroom  
714 productivity and phenology. *Frontiers in Ecology and the Environment*, 10(1), 14–  
715 19. doi:10.1890/110064
- 716 Büntgen U, Peter M, Kauserud H, Egli S (2013) Unraveling environmental drivers of a  
717 recent increase in Swiss fungi fruiting. *Global Change Biology*, 19(9), 2785–2794.  
718 doi:10.1111/gcb.12263

719 Chen T, Guestrin C (2016) KDD '16: Proceedings of the 22nd ACM SIGKDD  
720 International Conference on Knowledge Discovery and Data Mining, August 2016,  
721 Pages 785–794 doi:10.1145/2939672.2939785

722 Chen T, He T, Benesty M, Khotilovich V, Tang Y, Cho H, ... Li Y (2019) xgboost:  
723 Extreme Gradient Boosting. R package version 0.90.0.2. [https://CRAN.R-](https://CRAN.R-project.org/package=xgboost)  
724 [project.org/package=xgboost](https://CRAN.R-project.org/package=xgboost)

725 Christin S, Hervet É, Lecomte N (2019) Applications for deep learning in ecology.  
726 *Methods Ecol Evol*, 10:1632–1644. doi:10.1111/2041- 210X.13256

727 Coelho MTP, Diniz- Filho JA, Rangel TF (2018) A parsimonious view of the parsimony  
728 principle in ecology and evolution. *Ecography*. doi:10.1111/ecog.04228

729 Collado E, Camarero JJ, Martínez de Aragón J, Pemán J, Bonet JA, de-Miguel S (2018)  
730 Linking fungal dynamics, tree growth and forest management in a Mediterranean  
731 pine ecosystem. *Forest Ecology and Management*, 422, 223–232.  
732 doi:10.1016/j.foreco.2018.04.025

733 Collado E, Bonet JA, Camarero JJ, Egli S, Peter M, Salo K, ... de-Miguel S (2019)  
734 Mushroom productivity trends in relation to tree growth and climate across different  
735 European forest biomes. *Science of The Total Environment*.  
736 doi:10.1016/j.scitotenv.2019.06.471

737 Commission of the European Community. (1991) CORINE biotopes manual – Habitats  
738 of the European Community. Luxembourg: DG Environment, Nuclear Safety and  
739 Civil Protection.

740 Cortes C, Vapnik V (1995) Support-vector networks. *Machine Learning*, 20(3), 273–297.  
741 doi:10.1007/bf00994018

- 742 Cutler DR, Edwards TC, Beard KH, Cutler A, Hess KT, Gibson J, Lawler JJ (2007)  
743 Random forests for classification in ecology. *Ecology*, 88: 2783-2792.  
744 doi:10.1890/07-0539.1
- 745 De Cáceres M, Martin-StPaul N, Turco M, Cabon A, Granda V (2018) Estimating daily  
746 meteorological data and downscaling climate models over landscapes.  
747 *Environmental Modelling & Software*, 108, 186–196.  
748 doi:10.1016/j.envsoft.2018.08.003
- 749 de-Miguel S, Bonet JA, Pukkala T, Martínez de Aragón J (2014) Impact of forest  
750 management intensity on landscape-level mushroom productivity: A regional model-  
751 based scenario analysis. *Forest Ecology and Management*, 330, 218–227.  
752 doi:10.1016/j.foreco.2014.07.014
- 753 Diamantopoulou MJ, Özçelik R, Crecente-Campo F, Eler Ü (2015) Estimation of Weibull  
754 function parameters for modelling tree diameter distribution using least squares and  
755 artificial neural networks methods. *Biosyst. Eng.* 133:33–45.  
756 doi:10.1016/j.biosystemseng.2015.02.013
- 757 Dixon PA, Milicich MJ, Sugihara G (1999) Episodic Fluctuations in Larval Supply.  
758 *Science*, 283(5407), 1528–1530. doi:10.1126/science.283.5407.1528
- 759 Ehrlén J, Morris WF (2015) Predicting changes in the distribution and abundance of  
760 species under environmental change. *Ecology Letters*, 18(3), 303–314.  
761 doi:10.1111/ele.12410
- 762 Friedman J, Hastie T, Tibshirani R (2000) Additive logistic regression: a statistical view  
763 of boosting (With discussion and a rejoinder by the authors). *The Annals of Statistics*,  
764 28(2), 337–407. doi:10.1214/aos/1016218223

- 765 Gange AC, Gange EG, Sparks TH, Boddy L (2007) Rapid and Recent Changes in Fungal  
766 Fruiting Patterns. *Science*, 316(5821), 71–71. doi:10.1126/science.1137489
- 767 Gasch CK, Hengl T, Gräler B, Meyer H, Magney TS, Brown DJ (2015) Spatio-temporal  
768 interpolation of soil water, temperature, and electrical conductivity in 3D + T: The  
769 Cook Agronomy Farm data set. *Spatial Statistics*, 14, 70–90.  
770 doi:10.1016/j.spasta.2015.04.001
- 771 Gauch HG, Hwang JTG, Fick GW (2003) Model Evaluation by Comparison of Model-  
772 Based Predictions and Measured Values. *Agronomy Journal*, 95(6), 1442.  
773 doi:10.2134/agronj2003.1442
- 774 Georganos S, Abdi AM, Tenenbaum DE, Kalogirou S (2017) Examining the NDVI-  
775 rainfall relationship in the semi-arid Sahel using geographically weighted regression.  
776 *Journal of Arid Environments*, 146, 64–74. doi:10.1016/j.jaridenv.2017.06.004
- 777 Glassman SI, Wang IJ, Bruns TD (2017) Environmental filtering by pH and soil nutrients  
778 drives community assembly in fungi at fine spatial scales. *Mol. Ecol.*, 26, pp. 6960-  
779 6973. doi:10.1111/mec.14414
- 780 Gobeyn S, Mouton AM, Cord AF, Kaim A, Volk M, Goethals PLM (2019) Evolutionary  
781 algorithms for species distribution modelling: A review in the context of machine  
782 learning. *Ecological Modelling*, 392, 179–195.  
783 doi:10.1016/j.ecolmodel.2018.11.013
- 784 Görgens EB, Montaghi A, Rodriguez LCE (2015) A performance comparison of machine  
785 learning methods to estimate the fast-growing forest plantation yield based on laser  
786 scanning metrics. *Computers and Electronics in Agriculture*, 116, 221–227.  
787 doi:10.1016/j.compag.2015.07.004

- 788 Hamilton Jr D A, Brickell JE (1983) Modeling methods for a two-state system with  
789 continuous responses. *Canadian Journal of Forest Research*, 13(6), 1117–1121.  
790 doi:10.1139/x83-149
- 791 Hannemann H, Willis KJ, Macias-Fauria M (2015) The devil is in the detail: unstable  
792 response functions in species distribution models challenge bulk ensemble  
793 modelling. *Global Ecology and Biogeography*, 25(1), 26–35. doi:10.1111/geb.12381
- 794 Hao T, Guillera-Arroita G, May TW, Lahoz-Monfort JJ, Elith J (2020) Using Species  
795 Distribution Models for fungi. *Fungal Biology Reviews*.  
796 doi:10.1016/j.fbr.2020.01.002
- 797 Hastie T, Tibshirani R, Friedman J (2001) *The Elements of Statistical Learning: Data*  
798 *Mining, Inference, and Prediction*. New York: Springer-Verlag. ISBN 0-387-95284-  
799 5
- 800 Hill L, Hector A, Hemery G, Smart S, Tanadini M, Brown N (2017) Abundance  
801 distributions for tree species in Great Britain: A two-stage approach to modeling  
802 abundance using species distribution modeling and random forest. *Ecology and*  
803 *Evolution*, 7: 1043–1056. doi:10.1002/ece3.2661
- 804 Hughes G (1968) On the mean accuracy of statistical pattern recognizers. *IEEE*  
805 *Transactions on Information Theory*, 14(1), 55–63. doi:10.1109/tit.1968.1054102
- 806 James G, Witten D, Hastie T, Tibshirani R (2013) *An Introduction to Statistical Learning*.  
807 Springer Texts in Statistics. doi:10.1007/978-1-4614-7138-7
- 808 Juel A, Groom GB, Svenning J-C, Ejrnæs R (2015) Spatial application of Random Forest  
809 models for fine-scale coastal vegetation classification using object based analysis of

810 aerial orthophoto and DEM data. *International Journal of Applied Earth Observation*  
811 *and Geoinformation*, 42, 106–114. doi:10.1016/j.jag.2015.05.008

812 Karavani A, De Cáceres M, Martínez de Aragón J, Bonet JA, de-Miguel S (2018) Effect  
813 of climatic and soil moisture conditions on mushroom productivity and related  
814 ecosystem services in Mediterranean pine stands facing climate change. *Agricultural*  
815 *and Forest Meteorology*, 248, 432–440. doi:10.1016/j.agrformet.2017.10.024

816 Kauserud H, Stige LC, Vik JO, Okland RH, Hoiland K, Stenseth NC (2008) Mushroom  
817 fruiting and climate change. *Proceedings of the National Academy of Sciences*,  
818 105(10), 3811–3814. doi:10.1073/pnas.0709037105

819 Kauserud H, Heegaard E, Semenov MA, Boddy L, Halvorsen R, Stige LC, ... Stenseth,  
820 NC (2009) Climate change and spring-fruited fungi. *Proceedings of the Royal*  
821 *Society B: Biological Sciences*, 277(1685), 1169–1177. doi:10.1098/rspb.2009.1537

822 Le Rest K, Pinaud D, Monestiez P, Chadoeuf J, Bretagnolle V (2014) Spatial leave-one-  
823 out cross-validation for variable selection in the presence of spatial autocorrelation.  
824 *Global Ecology and Biogeography*, 23(7), 811–820. doi:10.1111/geb.12161

825 Liang J, Crowther TW, Picard N, Wiser S, Zhou M, Alberti G, ... Pretzsch H (2016)  
826 Positive biodiversity-productivity relationship predominant in global forests.  
827 *Science*, 354(6309), aaf8957–aaf8957. doi:10.1126/science.aaf8957

828 Liaw A, Wiener M (2002) Classification and Regression by randomForest. *R News* 2(3),  
829 18--22

830 Martínez de Aragón J, Bonet JA, Fischer CR, Colinas C (2007) Productivity of  
831 ectomycorrhizal and selected edible saprotrophic fungi in pine forests of the pre-  
832 Pyrenees mountains, Spain: Predictive equations for forest management of

833 mycological resources. *Forest Ecology and Management*, 252(1-3), 239–256.  
834 doi:10.1016/j.foreco.2007.06.040

835 Mayfield H, Smith C, Gallagher M, Hockings M (2020) Considerations for selecting a  
836 machine learning technique for predicting deforestation. *Environmental Modelling  
837 Software*, 104741. doi:10.1016/j.envsoft.2020.104741

838 Meyer H, Reudenbach C, Hengl T, Katurji M, Nauss T (2018) Improving performance of  
839 spatio-temporal machine learning models using forward feature selection and target-  
840 oriented validation. *Environmental Modelling Software*, 101, 1–9.  
841 doi:10.1016/j.envsoft.2017.12.001

842 Meyer H, Reudenbach C, Wöllauer S, Nauss T. (2019a) Importance of spatial predictor  
843 variable selection in machine learning applications – Moving from data reproduction  
844 to spatial prediction. *Ecological Modelling*, 411, 108815.  
845 doi:10.1016/j.ecolmodel.2019.108815

846 Meyer D, Dimitriadou E, Hornik K, Weingessel A, Leisch F (2019b) e1071: Misc  
847 Functions of the Department of Statistics, Probability Theory Group (Formerly:  
848 E1071), TU Wien. R package version 1.7-2. [https://CRAN.R-  
849 project.org/package=e1071](https://CRAN.R-project.org/package=e1071)

850 Micheletti N, Foresti L, Robert S, Leuenberger M, Pedrazzini A, Jaboyedoff M, Kanevski  
851 M (2013) Machine Learning Feature Selection Methods for Landslide Susceptibility  
852 Mapping. *Mathematical Geosciences*, 46(1), 33–57. doi:10.1007/s11004-013-9511-  
853 0

854 Mohan JE, Cowden CC, Baas P, Dawadi A, Frankson PT, Helmick K, ... Witt CA (2014)  
855 Mycorrhizal fungi mediation of terrestrial ecosystem responses to global change:  
856 mini-review. *Fungal Ecology*, 10, 3–19. doi:10.1016/j.funeco.2014.01.005

857 Olden JD, Lawler JJ, Poff NL (2008) Machine Learning Methods Without Tears: A  
858 Primer for Ecologists. *The Quarterly Review of Biology*, 83(2), 171–193.  
859 doi:10.1086/587826

860 Özçelik R, Diamantopoulou MJ, Crecente-Campo F, Eler U (2013) Estimating Crimean  
861 juniper tree height using nonlinear regression and artificial neural network models.  
862 *Forest Ecology and Management*. 306, 52–60. doi:10.1016/j.foreco.2013.06.009

863 Pinheiro JC, Bates DM (2000) *Mixed-effects models in S and S-PLUS*. First ed. Springer,  
864 New York. doi:10.1007/b98882

865 Pohjankukka J, Pahikkala T, Nevalainen P, Heikkonen J (2017) Estimating the prediction  
866 performance of spatial models via spatial k-fold cross validation. *International*  
867 *Journal of Geographical Information Science*, 31(10), 2001–2019.  
868 doi:10.1080/13658816.2017.1346255

869 Prasad A, Iverson L, Liaw A (2006) Newer Classification and Regression Tree  
870 Techniques: Bagging and Random Forests for Ecological Prediction. *Ecosystems* 9  
871 (2): 181–199. doi:10.1007/s10021-005-0054-1

872 Prasad AM (2018) Machine Learning for Macroscale Ecological Niche Modeling - a  
873 Multi-Model, Multi-Response Ensemble Technique for Tree Species Management  
874 Under Climate Change. *Machine Learning for Ecology and Sustainable Natural*  
875 *Resource Management*, 123–139. doi:10.1007/978-3-319-96978-7\_6

876 Propastin PA (2009) Spatial non-stationarity and scale-dependency of prediction  
877 accuracy in the remote estimation of LAI over a tropical rainforest in Sulawesi,  
878 Indonesia. *Remote Sensing of Environment*, 113(10), 2234–2242.  
879 doi:10.1016/j.rse.2009.06.007

880 Roberts DR, Bahn V, Ciuti S, Boyce MS, Elith J, Guillera-Arroita G, Dormann CF (2017)  
881 Cross-validation strategies for data with temporal, spatial, hierarchical, or  
882 phylogenetic structure. *Ecography*, 40(8), 913–929. doi:10.1111/ecog.02881

883 Sánchez-González M, de-Miguel S, Martín-Pinto P, Martínez-Peña F, Pasalodos-Tato M,  
884 Oria-de-Rueda JA, ... Bonet JA (2019) Yield models for predicting aboveground  
885 ectomycorrhizal fungal productivity in *Pinus sylvestris* and *Pinus pinaster* stands of  
886 northern Spain. *Forest Ecosystems*, 6(1) doi:10.1186/s40663-019-0211-1

887 Schratz P, Muenchow J, Iturrutxa E, Richter J, Brenning A (2019) Hyperparameter tuning  
888 and performance assessment of statistical and machine-learning algorithms using  
889 spatial data. *Ecological Modelling*, 406, 109–120.  
890 doi:10.1016/j.ecolmodel.2019.06.002

891 Sing T, Sander O, Beerenwinkel N, Lengauer T (2005) ROCr: visualizing classifier  
892 performance in R. *Bioinformatics*, 21(20), pp. 7881. <http://rocr.bioinf.mpi-sb.mpg.de>

893 Shmueli G (2010) To explain or to predict? *Statistical Science* 25(3), 289-310  
894 doi:10.1214/10-STS330

895 Smoliński S, Radtke K (2016) Spatial prediction of demersal fish diversity in the Baltic  
896 Sea: comparison of machine learning and regression-based techniques. *ICES Journal*  
897 *of Marine Science: Journal Du Conseil*, fsw136. doi:10.1093/icesjms/fsw136

898 Snowdon P (1991) A ratio estimator for bias correction in logarithmic regressions.  
899 *Canadian Journal of Forest Research*, 21(5), 720–724. doi:10.1139/x91-101

900 Stojanova D, Panov P, Gjorgjioski V, Kobler A, Džeroski S (2010) Estimating vegetation  
901 height and canopy cover from remotely sensed data with machine learning.  
902 *Ecological Informatics*, 5(4), 256–266. doi:10.1016/j.ecoinf.2010.03.004

903 Stokland JN, Siitonen J, Jonsson BG (2012) Biodiversity in Dead Wood, Biodiversity in  
904 Dead Wood. Cambridge University Press, Cambridge.  
905 doi:10.1017/CBO9781139025843

906 Taye ZM, Martínez-Peña F, Bonet JA, Martínez de Aragón J, de-Miguel S (2016)  
907 Meteorological conditions and site characteristics driving edible mushroom  
908 production in Pinus pinaster forests of Central Spain. Fungal Ecology, 23, 30–41.  
909 doi:10.1016/j.funeco.2016.05.008

910 Thessen A (2016) Adoption of Machine Learning Techniques in Ecology and Earth  
911 Science. One Ecosystem, 1: e8621. doi:10.3897/oneeco.1.e8621

912 Thornton PE, Running SW, White MA (1997) Generating surfaces of daily  
913 meteorological variables over large regions of complex terrain. Journal of  
914 Hydrology, 190(3-4), 214–251. doi:10.1016/s0022-1694(96)03128-9

915 Thornton PE, Running SW (1999) An improved algorithm for estimating incident daily  
916 solar radiation from measurements of temperature, humidity, and precipitation.  
917 Agricultural and Forest Meteorology, 93(4), 211–228. doi:10.1016/s0168-  
918 1923(98)00126-9

919 Thuiller W (2003) BIOMOD - optimizing predictions of species distributions and  
920 projecting potential future shifts under global change. Global Change Biology, 9  
921 (10), 1353– 1362. doi:10.1046/j.1365-2486.2003.00666.x

922 Toloşi L, Lengauer T (2011) Classification with correlated features: unreliability of  
923 feature ranking and solutions. Bioinformatics, 27(14), 1986–1994.  
924 doi:10.1093/bioinformatics/btr300

925 Valavi R, Elith J, Lahoz-Monfort JJ, Guillerá-Arroita G (2018) blockCV: an R package  
926 for generating spatially or environmentally separated folds for k-fold cross-validation  
927 of species distribution models. *Methods in Ecology and Evolution*.  
928 doi:10.1111/2041-210x.13107

929 Wheeler DC, Páez A (2009) Geographically Weighted Regression. In: Fischer M, Getis  
930 A. (eds) *Handbook of Applied Spatial Analysis*. Springer, Berlin, Heidelberg.  
931 doi:10.1007/978-3-642-03647-7\_22

932 Wood SN, Thomas MB (1999) Super-sensitivity to structure in biological models. *Proc*  
933 *R Soc Lond B Biol Sci* 266(1419):565–570. doi:10.1098/rspb.1999.0673

934 Ye H, Beamish RJ, Glaser SM, Grant SC, Hsieh C, Richards LJ, Schnute JT, Sugihara G  
935 (2015) Equation-free mechanistic ecosystem forecasting using empirical dynamic  
936 modeling. *Proceedings of the National Academy of Sciences*, 112:E1569–1576  
937 doi:10.1073/pnas.1417063112

938

939

940

941

942

943

944

945

946

947 **Supplementary Material**

948 3.1 Fitted models

949 3.1.1 Statistical models

950 Here we show the fitted GLMM and GWR models (coefficients are in Table S1 to S3) It  
 951 should be noted that the coefficients of GLMM and GWR are particular and different  
 952 from the general form of the conditioned mushroom production (S1) and the logit  
 953 transformation of the logistic regression (S2)

954  $\ln(prod) = \beta_0 + \beta_1 \ln(P_{aug+sep+oct}) + \beta_2 \ln(Tmax_{set})$  (S1)

955  $g = \beta_3 + \beta_4 \ln(P_{aug+sep+oct}) + \beta_5 Tmax_{oct}$  (S2)

956

957 Table S1. Fixed GLMM coefficients.  $\beta_1, \beta_2, \beta_3$  significance were calculated from t-  
 958 value, while  $\beta_3, \beta_4, \beta_5$  from p-value.

Coefficients	Estimate	Std. Error	Significance
$\beta_0$	2.858	2.203	1.298
$\beta_1$	1.048	0.156	6.680
$\beta_2$	-1.535	0.628	-2.442
$\beta_3$	6.437	4.999	0.198
$\beta_4$	2.149	0.598	0.000
$\beta_5$	-2.591	0.961	0.007

959

960

961

962 Table S2. Random GLMM coefficients.

Coefficient	Minimum	1 <sup>st</sup> quantile	Median	3 <sup>rd</sup> quantile	Maximum
$\beta_0$	-1.748	-0.408	0.096	0.425	1.323
$\beta_3$	-2.043	-0.395	0.359	0.821	1.363

963

964 Table S3. GWR models coefficients.

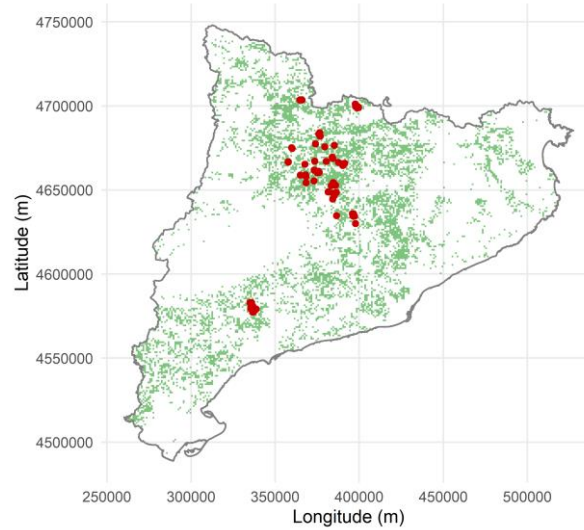
Coefficient	Minimum	1 <sup>st</sup> quantile	Median	3 <sup>rd</sup> quantile	Maximum
$\beta_0$	-4.207	-2.932	-0.612	0.298	0.980
$\beta_1$	1.439	1.580	1.738	2.231	2.636
$\beta_2$	-2.233	-1.724	-1.482	-1.398	-0.786
$\beta_3$	-7.908	-5.375	1.853	7.018	29.509
$\beta_4$	0.736	1.177	1.830	2.610	3.517
$\beta_5$	-7.096	-1.775	-1.453	-1.261	-0.654

Table S4. Model error in terms of root mean squared error (RMSE) and mean squared error (MSE) and his decomposition in squared bias (SB), nonunity slope (NU) and lack of correlation (LC) for random forest models (RF), extreme gradient (XGB), support vector machine (SVM), deep learning (DL), generalized linear mixed models (GLMM) and geographically weighted regression (GWR) models trained with 5 (.5) and 15 (.15) variables.

Blocking	% testing data	Parameter	RF.5	RF.15	XGB.5	XGB.15	SVM.5	SVM.15	DL.5	DL.15	GLMM	GWR
Random Blocking	5	SB	3.79	17.74	201.47	210.37	484.1	223.31	5.55	22.26	3169	22.89
	5	NU	99.25	81.29	29.6	105.46	5.14	43.37	0.25	3.87	2078.3	1544.68
	5	LC	12306.74	11138.82	12133.91	11405.9	13056.35	12560.4	14896.03	14741.47	15819.7	14416.35
	5	MSE	12409.78	11237.85	12364.98	11721.73	13545.59	12827.08	14901.83	14767.61	21067.01	15983.93
	5	RMSE	113.59	105.24	118.59	114.65	122.94	116.26	132.04	131.35	153.19	130.1
	10		113.52	108.54	118.02	114.32	119.78	116.8	127.88	127.01	147.92	127.35
	20		113.29	108.22	117.89	114.29	117.15	114.78	125.64	124.72	144.19	127.84
Spatial Blocking	5		139.13	133.9	149.22	136.4	137.64	138.06	140.59	136.49	166.95	153.48
	10		123.75	122.6	128.98	126.96	133.67	135.66	125.32	125.12	138.22	134.84
	20		124.18	124.84	128.66	126.52	135.65	137.63	126.39	126.04	135.1	133.93
Climate Blocking	5	111.46	110.24	114.96	111.97	120.08	116.51	115.7	115.6	128.12	128.52	
	10	128.3	126.13	137.36	129.71	144.76	133.88	130.8	132.37	143.22	142.02	
	20	123.17	121.73	126.92	126.13	133.99	129.01	126.74	127.46	134.44	134.91	
Substitution	5	58.83	51.58	88.41	81.87	105.97	84.12	124.38	123.5	143.73	128.01	

966 **Supplementary figures**

967

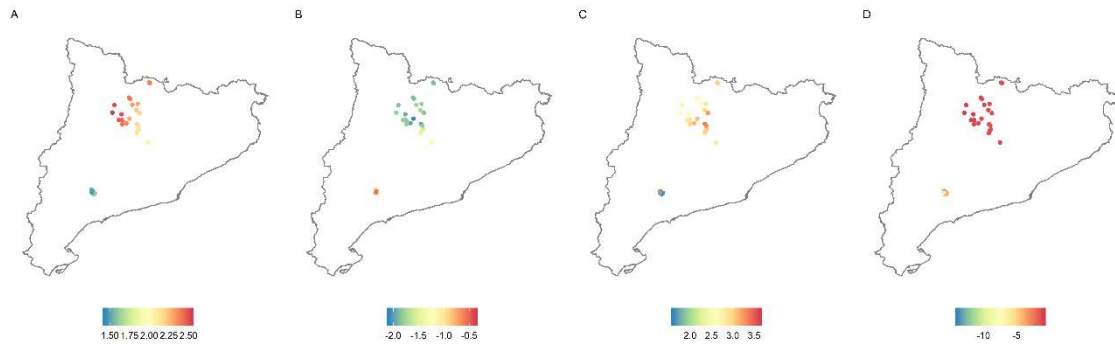


968 Figure S1. Study area, distribution of mushroom productivity monitoring plots (red  
969 points) and pine forest ecosystems represented by the sample plots (green area)  
970 Coordinates system: WGS 84 / UTM zone 31N.

971

972

973



974 Figure S2. GWR coefficient estimates according to geographical location. Coefficient of  
 975 precipitation amount from August to October (A) and maximum temperature in August  
 976 (B) in conditioned production model. Coefficient of precipitation amount from August to  
 977 October (A) and maximum temperature in October (D) in occurrence model (C).

978

979

980

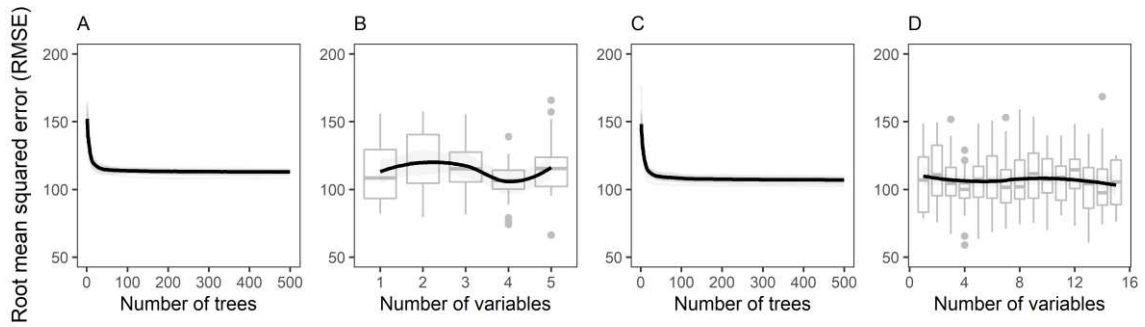
981

982

983

984

985



986

987 Figure S3. Hyperparameters selection for Random forest algorithm. (A) and (B)  
 988 corresponds to random forest models trained with 5 variables while (C) and (D)  
 989 trained with 15. For the trained models with 5 and 15 variables we chose 200 trees per  
 990 each model and 1 and 5 variables to be chosen randomly in each division, respectively.

991

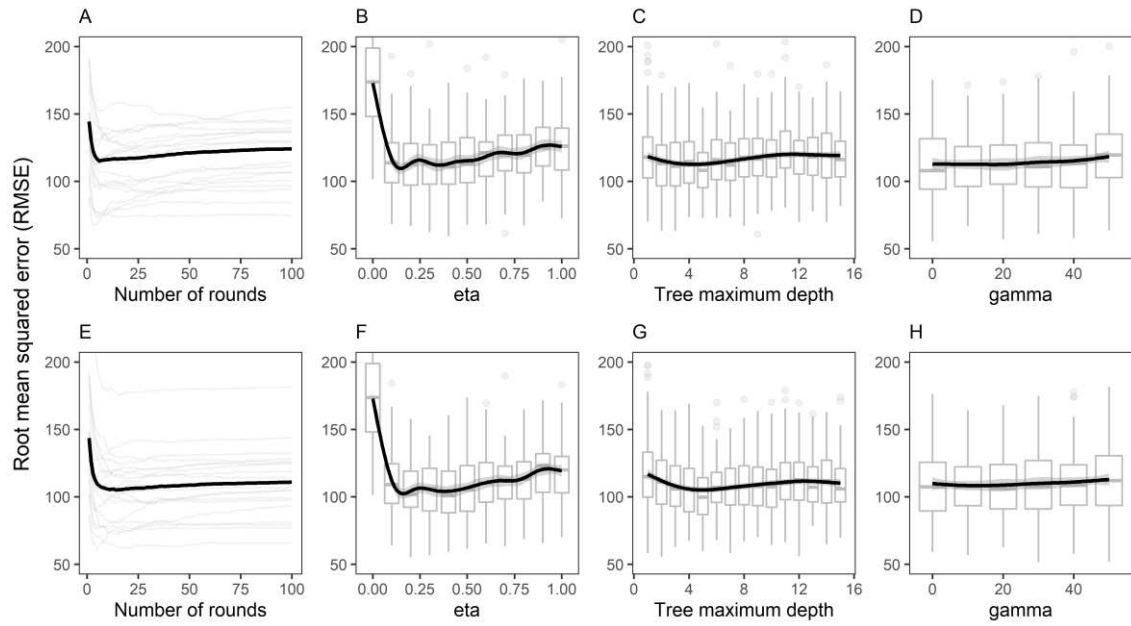
992

993

994

995

996



997

998 Figure S4. Hyperparameters selection for Extreme gradient boosting algorithm. (A) to  
 999 (D) corresponds to extreme gradient boosting models trained with 5 variables white (E)  
 1000 to (H) to those trained with 15. We chose 20 number of rounds and an eta of 0.1 for each  
 1001 model while choosing a depth of 5 and no regularization ( $\gamma=0$ ).

1002

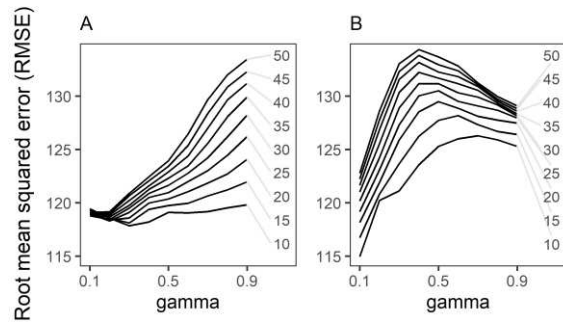
1003

1004

1005

1006

1007



1008

1009 Figure S5. Hyperparameters selection for Support vector machine algorithm. Different  
 1010 lines correspond to the value of the hyperparameter cost. (A) refers to support vector  
 1011 machine models trained with 5 variables while (B) to those trained with 15. We chose a  
 1012 gamma value of 0.3 and a cost of 10 for the 5-variable model while 0.1 and 10 respectively  
 1013 for the 15-variable model.

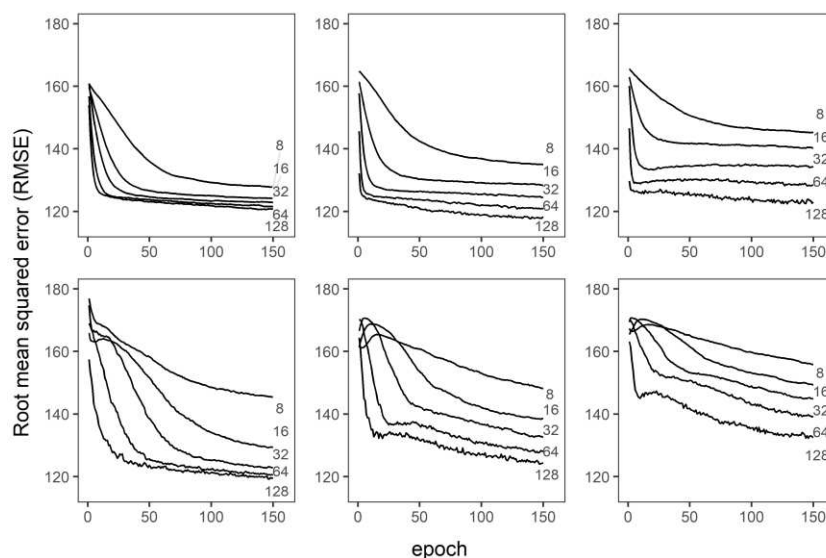
1014

1015

1016

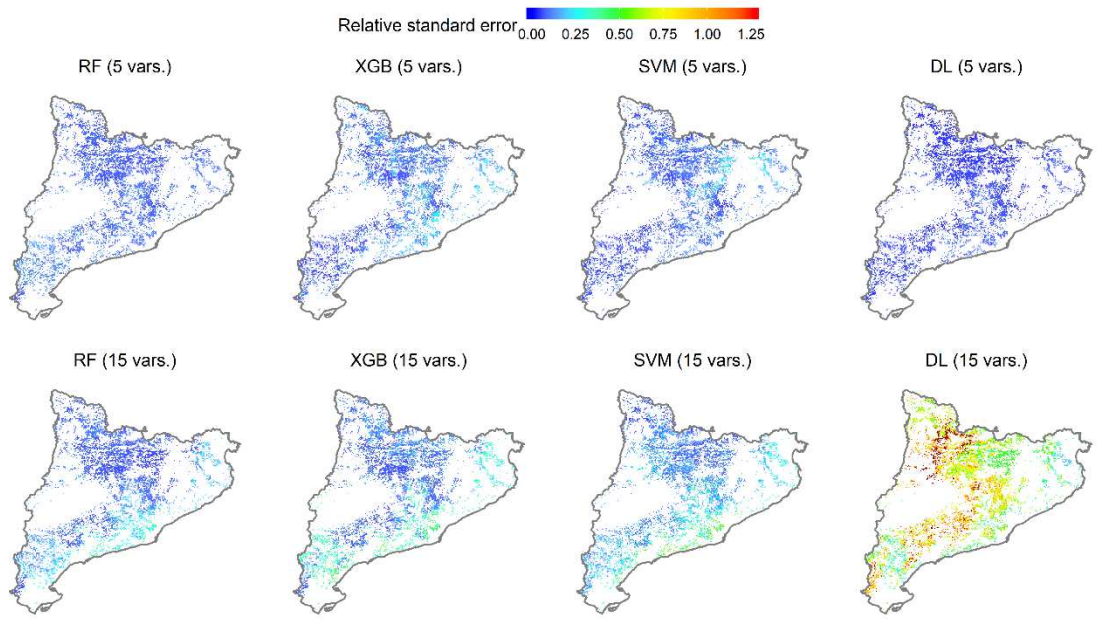
1017

1018



1019

1020 Figure S6. Hyperparameters selection for Deep learning algorithm. (A) to (C) refers to  
 1021 deep learning models trained with 5 variables while (D) to (F) to those trained with 15.  
 1022 (A) and (D) show ferments per 1 each with an activation function "relu" while (B) and  
 1023 (E) 2 and (C) and (F) 3. A final layer with a single output value and a "relu" activation  
 1024 function is added to all of them. In between each layer a dropout layer has been added  
 1025 which randomly selects 50% of the data for training. The different lines of each graph  
 1026 show the dimensionality of the output space.



1027 Figure S7. Spatially explicit standard error map of the 50 model estimations

# Figures

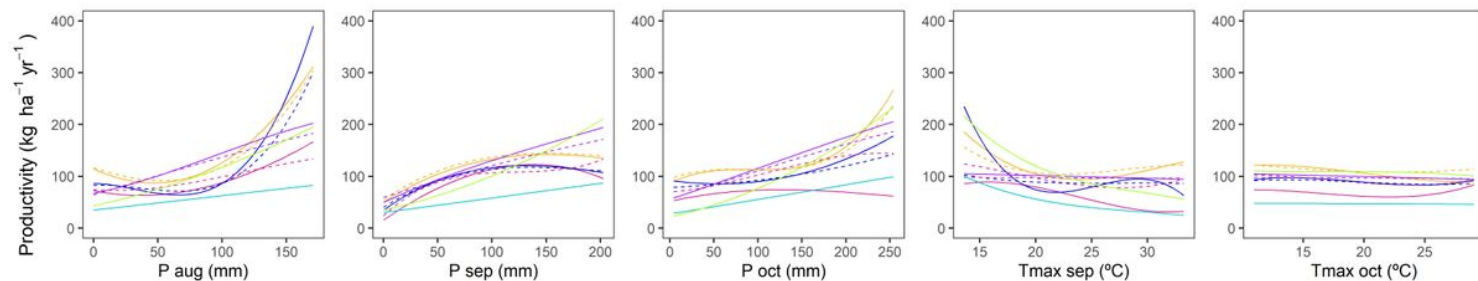


**Figure 1**

Relationship between annual mushroom productivity and August, September and October precipitation and maximum temperatures in September and October (these variables are the variables used in the statistical models and the five variables machine learning models). Yellow (random forest), blue (extreme gradient boosting), violet (support vector machine), purple (deep learning), light blue (generalized linear mixed models) and light green (geographically weighted regression) colours refer to the different modelling techniques. Continuous line includes the models that use the five variables and the dashed line the machine learning models trained with 15.

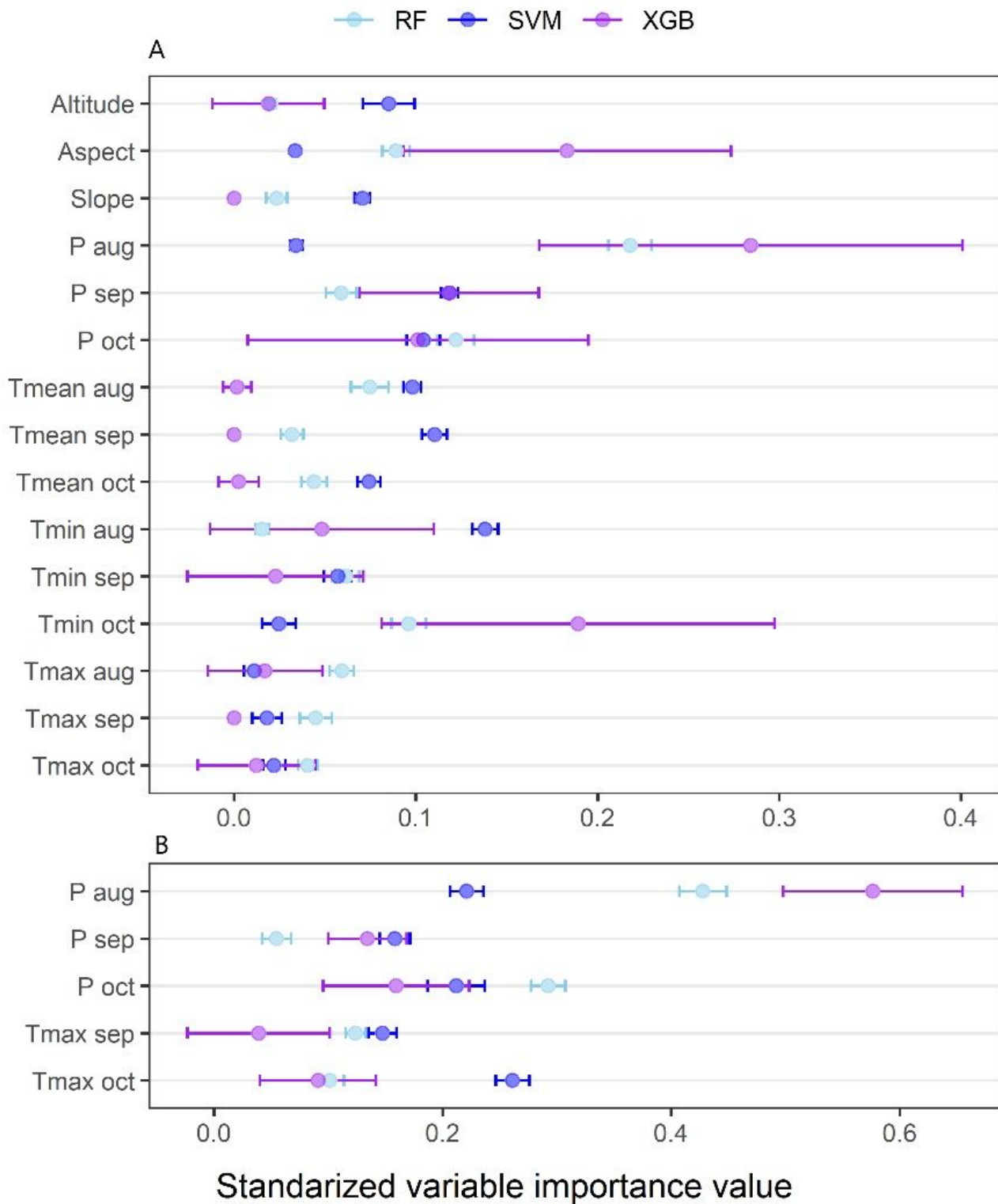


**Figure 2**

Standardized variable importance value used to train random forest (RF), extreme gradient boosting (XGB) and support vector machine (SVM) models with 15 (A) and 5 (B) variables. Variable importance values represent the contribution of each variable to predict the annual mushroom productivity.

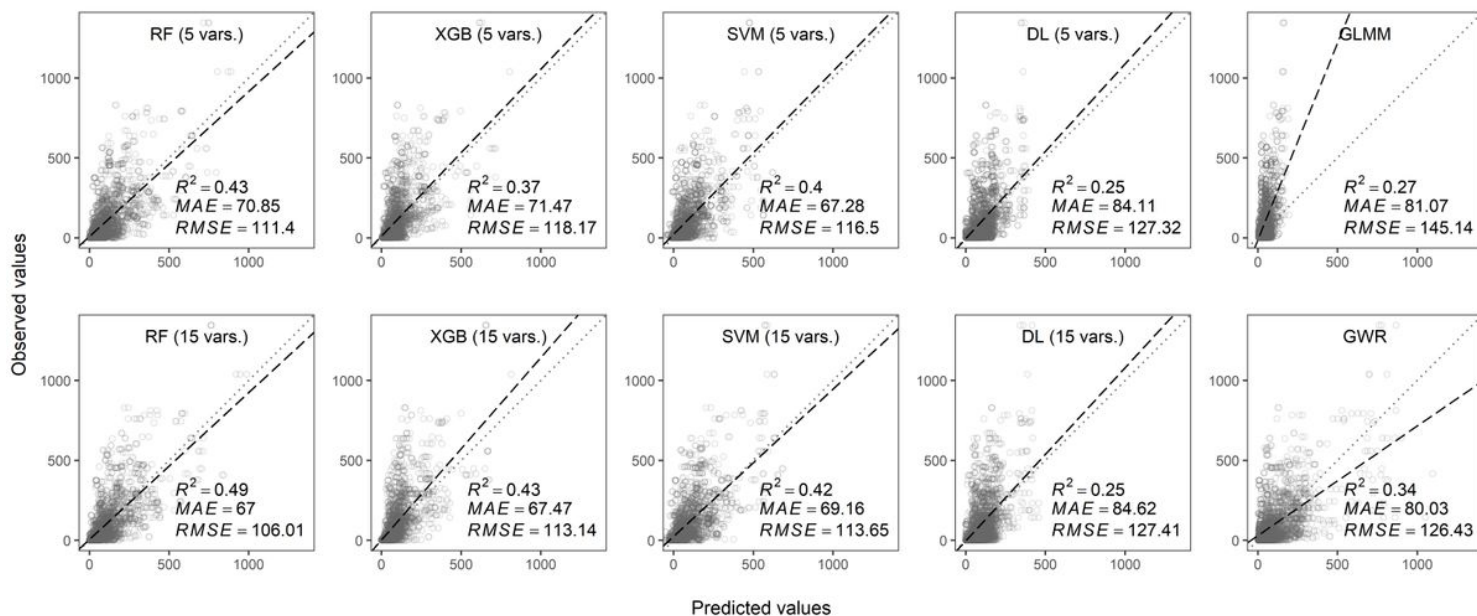


**Figure 3**

Cross-validation of estimated total mushroom production (kg ha<sup>-1</sup> year<sup>-1</sup>) using random forest (RF), extreme gradient boosting (XGB), support vector machine (SVM) and deep learning (DL) trained with 15 and 5 variables and generalized linear mixed models (GLMM) and geographically weighted regression (GWR). Pointed line shows the equality line and the dashed one the best fit between predicted and observed values. It shows mean absolute error (MAE), root-mean-squared error (RMSE) and coefficient of determination ( $R^2$ ) of the relation for each technique.

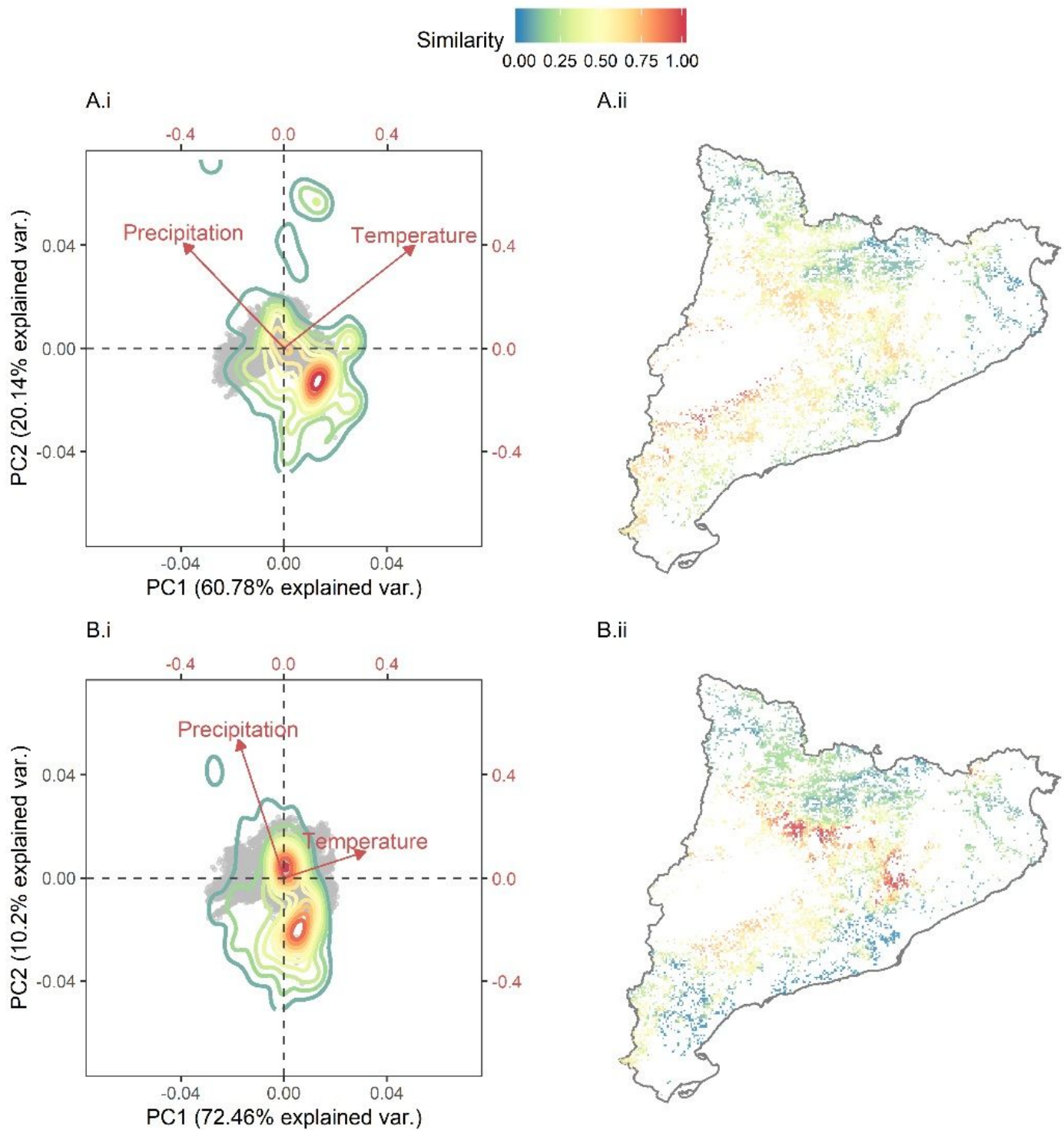


**Figure 4**

Similarity between the annual meteorological data of the sampled plots (used to train the models) and the average climatology of the Catalan pine forests (used to predict).

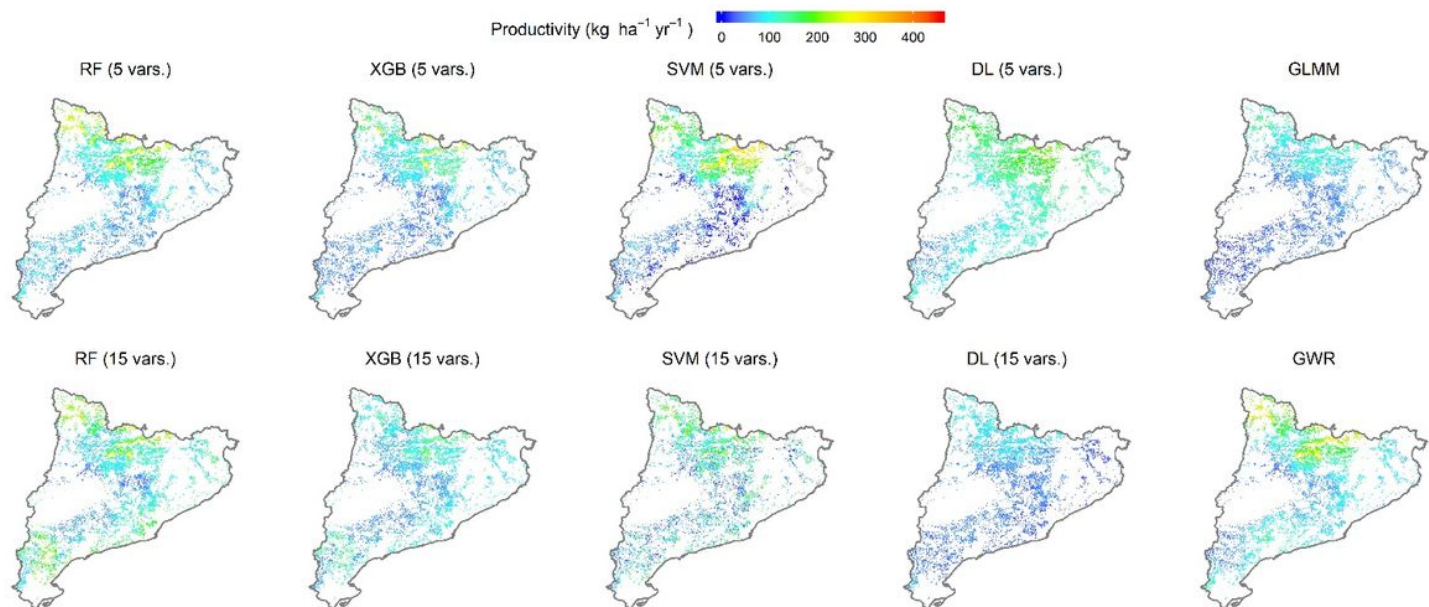


**Figure 5**

Landscape-level prediction of total annual mushroom productivity, using random forest (RF), extreme gradient boosting (XGB), support vector machine (SVM) and deep learning (DL) trained with 15 and 5 variables, respectively, and generalized linear mixed models (GLMM) and geographically weighted regression (GWR) fitted using 5 predictors.

## Supplementary Files

This is a list of supplementary files associated with this preprint. Click to download.

- [floatimage7.png](#)
- [floatimage8.png](#)
- [floatimage9.png](#)
- [Onlinefloatimage10.Png](#)
- [Onlinefloatimage11.Png](#)
- [Onlinefloatimage12.Png](#)
- [Onlinefloatimage13.Png](#)